International Journal of Biological Macromolecules 306 (2025) 141287

Contents lists available at ScienceDirect

International Journal of Biological Macromolecules

journal homepage: www.elsevier.com/locate/ijbiomac

Laminarins and their derivatives affect dendritic cell activation and their crosstalk with T cells

Monica Daugbjerg Christensen [a,b,c,*], Leila Allahgholi [d], Justyna M. Dobruchowska [e], Antoine Moenaert [a,f], Hörður Guðmundsson [a], Ólafur Friðjónsson [a], Eva Nordberg Karlsson [d], Guðmundur Ó. Hreggviðsson [a,f], Jona Freysdottir [c,g]

[a] Department of Biotechnology and Biomedicine, Matís ohf, Vínlandsleið 12, IS-113 Reykjavík, Iceland
[b] Faculty of Food Science and Nutrition, University of Iceland, Sæmundargata12, IS-102 Reykjavík, Iceland
[c] Department of Immunology, Landspitali—The National University Hospital of Iceland, IS-101 Reykjavik, Iceland
[d] Division of Biotechnology, Department of Chemistry, Lund University, PO Box 124, SE-221 00 Lund, Sweden
[e] Department of Chemical Biology and Drug Discovery, Utrecht Institute for Pharmaceutical Sciences, Bijvoet Center for Biomolecular Research, Utrecht University, Universiteitsweg 99, 3584 CG Utrecht, the Netherlands
[f] Faculty of Life and Environmental Sciences, University of Iceland, Sturlugata 7, IS-102 Reykjavík, Iceland
[g] Faculty of Medicine, Biomedical Center, University of Iceland, Vatnsmyrarvegur 16, IS-101 Reykjavik, Iceland

ARTICLE INFO

Keywords:
Laminarin structure
Dendritic cells
Allogeneic T-cells
Immunomodulating effects
Brown macroalgae

ABSTRACT

This research explores the impact of structural variations in laminarins derived from seaweed on their immunomodulatory properties. Laminarins from *Laminaria digitata*, *L. hyperborea*, and *Saccharina latissima,* were obtained using a two-step water extraction protocol, followed by structural characterization by FT-IR spectroscopy, ^{1}H NMR, and MALDI-TOF MS. The laminarin backbones were confirmed as β–1,3-linked glucans with species-specific percentages of β–1,6-linkages (~10 %, ~4 %, and ~21 %, respectively). Each polymer chain consists of approximately 24 to 25 monomer units, while oligosaccharide fractions, produced using the enzyme LPHase, displayed distinct DP-ranges, degrees of β–1,6-branching and intrachain linkages. Laminarin from *L. hyperborea* and specific oligosaccharide fractions from *L. hyperborea* and *S. latissima* influenced cytokine secretion by dendritic cells (DCs). *L. hyperborea* laminarin and the fraction *Lh*F5 (DP5–DP8) stimulated increased IL-6 and IL-10 secretion by DCs, suggesting a dual role in promoting inflammation and regulating the immune response. In contrast, *Lh*F5, *Lh*F4 (DP6–DP10), and *S. latissima* laminari-oligosaccharide fraction *Sl*F3 (DP6–DP9) caused decreased TNFα secretion, reflecting anti-inflammatory potential. Co-culturing of treated DCs and CD4^{+} T-cells showed that *L. hyperborea* laminarin caused increased IL-17 and IL-10 secretion, whereas *Sl*F3 caused reduced IL-12p40 and IFN-γ secretion. These findings show that DC maturation and T-cell activation are affected by laminarins of certain size-distribution and branching, implying therapeutic potential for the treatment of inflammatory diseases or vaccine enhancement.

1. Introduction

Brown seaweed, encompassing around 2000 different species, is a potentially rich source of health promoting compounds [1]. This has raised significant interest in studying their potential for medical purposes or as functional foods. One of the compounds of interest is laminarin, a low-molecular-weight storage polysaccharide (2–7 kDa), with a degree of polymerization (DP) in the range of 25–40 [2–4]. Laminarin is a water-soluble β-glucan, consisting of a β–1,3–D-glucose backbone, interspersed with β–1,6-linked glucose moieties [5]. The content and positioning of β–1,6 linkages in laminarins varies depending on the species, season, and environmental conditions [6]. The β–1,6-linkages can be internal in the linear β–1,3-backbone (intrachain) or form branch-points (branched β-glucan oligosaccharides) [3,7]. Furthermore, the laminarin glucan chains are capped at the reducing end with either mannitol or glucose moieties, referred to as M-chains and G-chains, respectively. The content and distribution of these two variants also varies among species [7,8].

* Corresponding author at: Department of Biotechnology and Biomedicine, Matís ohf, Vínlandsleið 12, IS-113 Reykjavík, Iceland.
E-mail address: monica@matis.is (M.D. Christensen).

https://doi.org/10.1016/j.ijbiomac.2025.141287
Received 11 December 2024; Received in revised form 28 January 2025; Accepted 17 February 2025
Available online 19 February 2025

Laminarin polysaccharides have been associated with a range of bioactive properties including: antioxidant, anti-inflammatory, anti-apoptotic, immunomodulation, and potential anti-cancer properties [4,9–13]. Due to their bioactivities, they are promising candidates for nutraceutical and pharmaceutical applications. However, the relation between structural features and biological functions of laminarin is not yet fully understood. Addressing this knowledge gap is critical for developing laminarin-based interventions, particularly for functional foods or therapies targeting immune-related disorders, such as inflammatory diseases, or enhancing vaccine efficacy. The bioactive properties of laminarin polysaccharides have been proposed to be associated with their structural features, such as DP, degree of branching (DB), and the ratio of β–1,3 to β–1,6-glycosidic linkages, but also affected by purity [4,5,11,14]. Conventional extraction methods for laminarin have often used acidic conditions, which can alter the compound's structure and potentially lead to inconsistent bioactivity results [15]. For example, treatment with 0.1 M hydrochloric acid has been shown to lower the DP of oat-derived β-glucan by breaking 1,3– and 1,4–β-linkages, thereby increasing the amounts of glucose and smaller oligosaccharides [16]. Additionally, mildly acidic conditions have been intentionally used to produce high-value oligosaccharides from *L. digitata*, leading to laminarin oligosaccharides with modified antioxidant and prebiotic properties [17]. Methods that introduce structural changes, also introduce challenges in relating structure to function, making it essential to determine detailed structures in the same batch as used for the documentation of the bioactivity. Further knowledge on the native laminarins, is also essential for rational choices of raw-material, to improve our understanding of which species produce relevant laminarins for specific applications. Moreover, existence of impurities and high ash content can result in misleading conclusions regarding bioactivities. This was documented in a study by Smith and colleagues (2018), where a laminarin sample was initially acting as a Dectin-1 antagonist, but after removing low molecular weight impurities it became a Dectin-1 agonist [4,5,11,14].

Recently, enzymatic digestion methods, using laminaripentaose-producing β–1,3-glucanases suitable for hydrolyzing laminarin into oligosaccharides, have been employed to elucidate more structural details in biomacromolecules like laminarin [5]. Liu and colleagues [5] applied this method combined with HPAEC-PAD-MS/MS analysis to, e.g., reveal the presence of β–1,6-linkages in laminarins from *L. digitata* and *Eisenia bicyclis*. This method can not only provide insight into the structural intricacies of laminarin but can also help to explore structure-function relationships of the produced oligosaccharides. Laminarin-degrading enzymes have, therefore been used to generate laminari-oligosaccharides to study bioactivities, including antioxidant, antidiabetic, and to a certain extent, immuno-modulating effects [7,12,18]. However, the relation between oligosaccharide structures and immunomodulating activities is still underexplored, and thus far no definite conclusions are drawn.

DCs are the key initiators of the adaptive immune response, by activating and polarizing naïve T-cell responses. In their immature state, they reside in tissues, functioning as sentinels scanning for danger signals [19,20]. When encountering foreign antigens, such as pathogen- or damage-associated molecular patterns (PAMPs or DAMPs), DCs activate and undergo phenotypic and functional changes transforming them into their mature stage. This maturation involves the up-regulation of surface molecules vital for antigen presentation, such as major histocompatibility complex (MHC) molecules, as well as the co-stimulatory molecules CD80 and CD86 [20]. Subsequently, mature DCs migrate to draining lymph nodes where they prime naïve T-cells, steering them toward becoming effector cells, including T-helper (Th)1, Th2, and Th17 subsets, or cytotoxic T-cells [21,22]. The repertoire of cytokines secreted by the mature DCs during this process depends on the PAMPs or DAMPs encountered [19,20].

Notably, the cytokines secreted by DCs orchestrate the downstream immune responses, such as IL-12 and IL-6, which direct the polarization of naïve $CD4^+$ T-cells into Th1 or Th17 effector cells, respectively [23,24]. However, IL-6 has a complex role in immune modulation, as reviewed in [25]. It is a pro-inflammatory cytokine critical for activating Th17 responses against extracellular pathogens and initiating acute inflammation, whereas it can also promote production of IL-10 by T cells, thus restricting inflammatory processes [25]. Simultaneous upregulation of IL-6 and IL-10 cytokine secretion can, therefore, be linked to anti-inflammatory responses. TNFα, is a potent pro-inflammatory cytokine, which plays a pivotal role in driving inflammation and the activation of immune cells [26,27]. However, its sustained production can contribute to chronic inflammation and tissue damage. This is observed in numerous autoimmune disorders, such as rheumatoid arthritis, inflammatory bowel disease, psoriatic arthritis and multiple sclerosis (reviewed [28], which respond well to anti-TNF therapy. IL-10 acts as a potent anti-inflammatory cytokine that suppresses the production of pro-inflammatory mediators (e.g., TNFα, IL-1β, IL-6) and reduces the expression of MHC and co-stimulatory molecules on DCs [29]. While extended production of IL-6 and TNFα initiates the recruitment and activation of immune effector cells, IL-10 counter-regulates these processes to mitigate excessive immune activation and restore homeostasis [29,30]. These mechanisms are in line with the complex effects of laminarin and its oligosaccharides on cytokine secretion observed in this study, reflecting both pro-inflammatory and regulatory capacities. Such immunomodulatory properties highlight their multiple potential in therapeutic applications, including the treatment of inflammatory diseases and immune-mediated disorders.

In this study, a mild two-step water extraction protocol was used for laminarin extraction. A temperature escalation approach was applied for effective isolation of laminarin. This method was chosen for its simplicity, eco-friendliness, and ability to avoid the use of residual solvents or chemical modifications, which is critical for applications in functional foods, pharmaceuticals, or nutraceuticals, where regulatory compliance and consumer safety are paramount. This approach not only preserves the structural integrity of laminarin but also simplifies the purification process, avoiding the need for additional reagents or complex downstream procedures. As mentioned, mildly acidic extraction conditions can alter laminarin's structure by breaking β-linkages, reducing the DP, resulting in production of altered structures with smaller oligosaccharides. In contrast, our protocol avoids such extremes, ensuring that the laminarin's structural and functional characteristics remain intact. Although alternative methods, such as enzymatic hydrolysis or ultrasound-assisted extraction, may offer higher yields or efficiency, these techniques often require additional reagents or specialized equipment, increasing both complexity and cost. High purity of the laminarins was ensured by including precipitation, filtration, and dialysis of the extracts from *L. digitata*, *L. hyperborea,* and *S. latissima*. The output, purity, DP and DB of the extracted laminarins were subsequently evaluated by high-performance anion exchange chromatography with pulsed amperometric detection (HPAEC-PAD), Fourier-transform infrared spectroscopy (FT-IR), proton nuclear magnetic resonance (^{1}H NMR), and Matrix-Assisted Laser Desorption/Ionization Time-of-Flight Mass Spectrometry (MALDI-TOF MS). Furthermore, the laminarins extracted from the aforementioned species were subjected to enzymatic hydrolysis to produce laminari-oligosaccharides of different sizes and DB. The hydrolysis process was executed using the laminaripentaose-producing endo-1,3–β-glucanase (LPHase) from *Streptomyces matensis* DIC-108 [31], in an attempt to create laminari-oligosaccharides with varied immunomodulating effect and facilitating a systematic exploration of their structure-function relationships. Given laminarin's structural complexity and species-specific variations, we hypothesize that its immunomodulatory effects are associated with distinct structural features, including DP, branching patterns, and β–1,6-linkage content, which may influence its interactions with immune cells. By utilizing a mild, non-degradative extraction method and precise enzymatic hydrolysis to produce laminari-oligosaccharides, this study aims to correlate these structural characteristics systematically with

immunomodulatory activities by exploring their impact on the maturation and activation of human monocyte-derived DCs, as well as the ability of laminarin- or laminari-oligosaccharide treated monocyte-derived DCs to activate and differentiate allogeneic $CD4^+$ T-cells. This is an innovative approach to bridging the existing knowledge gap concerning the structure-function relationships in laminarins, offering potential applications in developing laminarin-based nutraceuticals or therapeutic agents, for the context of treating inflammatory diseases or enhancing vaccine efficacy.

2. Material and method

2.1. Materials

Dried *S. latissima* was kindly provided by Annette Bruhn (Department of Bioscience at Aarhus University, AlgeCenter, Denmark). Similarly, dried *L. hyperborea* and *L. digitata* were provided by Íslensk Bláskel og Sjávargróður, Iceland. The samples were harvested during summer (2018) to assure high laminarin yields. Voucher specimens for *L. hyperborea* and *L. digitata* were deposited and are available for reference. Unfortunately, it was not possible to deposit a voucher specimen for *S. latissima*. The dried raw materials were stored in sealed bags, at room temperature, in the dark. Purified laminarin from *L. digitata* (harvested in Iceland) was also obtained from Merck (Darmstadt, Germany, Lot #SLCG6449), and was stored according to the manufacturer's instructions. The *S. latissima*, *L. hyperborea*, and the commercial *L. digitata* biomasses were used to generate the laminari-oligosaccharides fractions described in Section 2.4.2.

2.2. Laminarin extractions and purification

2.2.1. Extractions and filtration

Dried *L. hyperborea* and *S. latissima* were ground to a fine powder (~1 mm particle size) using an IKA® A10 mill. Crude laminarin was extracted with a two-step water protocol: 100 g of seaweed powder was mixed with 1.5 L distilled water, initially extracted at 30 °C for 2 h with continuous shaking (75 rpm), followed by extraction at 70 °C for 3 h. The cooled extracts (4 °C overnight) were centrifuged (~12,000*g* for 20 min) to separate pellets and supernatants. The pellets were recentrifuged to maximize yield.

Calcium chloride ($CaCl_2$) of 1 % was used at 4 °C overnight to precipitate alginate, a well-established method for isolating polysaccharides [32], followed by centrifugation (~12,000*g* for 20 min) to separate and discard the precipitated alginate pellet from the extract. For further purification, the clear laminarin extracts underwent filtration using the Cogent®10 M1 tangential flow filtration (TFF) system (Merck Millipore) equipped with 10 kDa filters. Subsequently, the extracts were further purified by dialysis on the TFF-system using 1 kDa filters. The extracts were lyophilized and stored at −20 °C until further use.

2.2.2. Separation of L. hyperborea-derived laminarin from fucoidan polysaccharides by anion-exchange chromatography

The extract from *L. hyperborea* (extracted as described in Section 2.2.1) required further purification to separate laminarin from fucoidan. A 10 mg dried extract sample was dissolved in 1 mL of distilled water and loaded onto a DEAE-cellulose column (1 × 20 cm; Sigma-Aldrich, St. Louis, MO, USA), equilibrated with distilled water. Laminarin fractions were eluted with water and lyophilized. The remaining material in the column was fucoidan (containing sulfate as anionic functional group), which was eluted with 1 M ammonium bicarbonate buffer.

2.3. Composition analyses and profiling of the laminarin polysaccharides

2.3.1. Total phenolic content (TPC)

Portions (100 mg) of lyophilized laminarin extracts were dissolved in 10 mL ultrapure water (Milli-Q grade) and vortexed until all the powder was dissolved. The total phenolic content was determined using the method published by Singleton and Rossi [33], adapted to a microplate format with some modifications. Briefly, 20 μL of the sample was mixed with 100 μL of 0.2 N Folin & Ciocalteu's phenol reagent (Sigma-Aldrich) and incubated at room temperature for 5 min. Then, 80 μL of 7.5 % Na_2CO_3 (Sigma-Aldrich) were added, and the mixture was heated for 10 s in microwave oven at 550 W. After heating, the mixture was incubated at room temperature for 30 min under constant agitation. Absorbance was read at 730 nm using a microplate reader (Thermo Scientific MultiSkan Sky with SkanIt software 6.0.1). A standard curve with seven concentrations of phloroglucinol was used, and results were expressed as mg of phloroglucinol equivalents (PGE) per 100 g of lyophilized laminarin extract, obtained through interpolation from regression analysis.

2.3.2. Ash content

Ash content was measured after combusting the moisture free powder at 550 °C for 10 h in a furnace [34]. All measurements were carried out in duplicates, and quantification was done gravimetrically.

2.3.3. Carbohydrate composition quantification and laminarin profiling

The carbohydrate composition of the water-extracted laminarin samples and the commercial sample was quantified using a two-step sulfuric acid hydrolysis, adjusted for algal biomass [35]. An amount of 25 mg of freeze-dried extracts was mixed with 250 μL of 72 % sulfuric acid in Pyrex tubes, and the samples were incubated at 30 °C for 1 h with shaking (150 rpm). Then, the acid was diluted to 4 % (*w/w*) by adding 7 mL of distilled water to the tubes and then the samples were autoclaved for 1 h at 121 °C (1 atm). The hydrolysates were cooled to room temperature and centrifuged at 3000 ×*g* for 5 min (Sigma 3–16PK centrifuge, Sigma), followed by neutralization of the supernatants with Ba$(OH)_2{\cdot}H_2O$ (0.1 M). Removal of precipitated residues was done by centrifugation at 3000 ×*g* for 5 min (Sigma 3–16PK centrifuge, Sigma). The neutralized hydrolysates were diluted and filtered through 0.2 μm PTFE syringe filters (Pall) and analyzed using HPAEC-PAD (Thermo Fisher Scientific), with a Dionex CarboPac PA-20 analytical column and a corresponding guard column (Thermo Fisher Scientific) for monosaccharide separation. The separation of monosaccharides and uronic acid was performed under isocratic conditions at a flow rate of 0.5 mL/min. Eluents for separation of monosaccharides and mannitol were (A) milliQ-water, (B) 2 mM NaOH, and (C) 200 mM NaOH. Separation was done using an eluent mixture of 62.5 % (A) and 37.5 % (B) for 30 min. For separation of uronic acids, eluent (B) was 1 M sodium acetate in 200 mM NaOH while eluents (A) and (C) were the same as for monosaccharide separation. The uronic acids were eluted by an eluent mixture of 55 % (A), 15 % (B) and 30 % (C) for 18 min. The column and the compartment temperature were kept at 30 °C. All the experiments were performed in duplicate, and the mean value and standard deviation were calculated. Total carbohydrates were estimated as the sum of all individual monomeric sugars.

2.4. Enzymatic generation of laminari-oligosaccharides

2.4.1. Expression of the lph gene and production of recombinant LPHase in Escherichia coli

The sequence for LPHase (encoding 376 amino acids) was obtained from *Streptomyces matensis* DIC-108, as previously described [31], and was extended with a maltose-binding protein domain (MalE) in the cloning design to enhance solubility. The gene was amplified using the forward primer f(CCATCGTGAACAGATTGGTGGCGCCGCCGTTCCAG CGACCATTC) and the reverse primer, r(TTAATGATGATGATGAT-GATGGG*GATCC*ATCGAACGGGTCCAGAGTCAG). The expression vector pHWG1106 [36] was linearized with *Kas*I and *Bam*HI and subsequently, the gene was inserted into the vector using the NEBuilder® HiFi DNA Assembly Cloning Kit (New England Biolabs Inc.). The resulting plasmid,

pHG247, was introduced into *E. coli* NEB10 beta competent cells by transformation. Expression was achieved by cultivating pHG247/NEB10 in 30 mL LB broth supplemented with ampicillin (100 μg/mL) at 37 °C until reaching an OD_{600} 0.7. The culture was then moved to room temperature and allowed to grow until reaching an OD_{600} of approximately 0.9. Gene expression was induced by adding 10 % (*w/v*) L-rhamnose, resulting in a final concentration of 0.15 %. The culture was incubated overnight at room temperature. Cells were harvested by centrifugation at 3,400*g* for 10 min at 4 °C (~0.3 g) and resuspended in four times the volume of lysis buffer (~1.2 mL; 50 mM sodium citrate, pH 6, 150 mM NaCl, 15 % glycerol). Cell disruption was achieved by sonication on ice. The cell lysate was centrifuged at 16,000*g* for 30 min at 4 °C to separate the supernatant from the insoluble debris. Expression of LPHase was confirmed by sodium dodecyl-sulfate polyacrylamide gel electrophoresis (SDS-PAGE), using Mini-PROTEAN® TGX Stain-Free™ Precast Gels (4–20 %, 15-well), in Tris-glycine-SDS (TGS) running buffer. The supernatant was stored as a crude extract at −80 °C until use in laminarin hydrolysis experiments.

2.4.2. Enzymatic laminarin hydrolysis and purification of laminari-oligosaccharide extracts

The enzymatic hydrolysis was conducted at 50 °C and pH 5.7, as optimized for LPHase activity. Simultaneously, dialysis was performed to separate the laminari-oligosaccharides from the substrate. The procedure was as follows: A 50 mL 4 % solution of lyophilized laminarin from *L. digitata*, *L. hyperborea* and *S. latissima* was prepared by mixing it with 20 mM sodium citrate buffer (pH 5.7). LPHase crude extract was added to the laminarin solutions at a volume of 200 μL, corresponding to approximately 1.2 mg per reaction. The mixtures were transferred into Slide-A-Lyzer® 3.5 K Dialysis cassettes G2 (Thermo Scientific) and placed in 1 L beakers. The beakers were filled to the 550 mL mark with 20 mM sodium citrate buffer (pH 5.7) and securely covered with plastic wrap and aluminum foil to prevent evaporation. The sealed beakers were incubated in a 50 °C in a heating cabinet for two days, with manual shaking 4 to 5 times daily throughout the incubation period. Upon completion, the surrounding buffer, containing the produced oligosaccharides, was collected for each reaction, frozen, and subsequently lyophilized to yield the desired product.

For the purification of the laminari-oligosaccharide mixtures, a 12 % (*w/v*) solution of lyophilized laminari-oligosaccharides from each species was prepared by mixing the extracted laminarins with milli-Q water. The solutions were filtered through non-sterile Phenex RC membrane (0.45 μm, 26 mm syringe filters; Phenomenex). Purification of the laminari-oligosaccharide mixtures was executed using an ÄKTA system with a size-exclusion Superdex™ 30 HiLoad 26/600 column (Cytiva). The column was equilibrated with a low ionic strength buffer (50 mM NaCl), and the running buffer was degassed milli-Q water. A total of 12 mL of the 12 % oligosaccharides solution, plus additional 5 mL of milli-Q water, was loaded onto the column. Separation was initiated by allowing 0.37 column volumes to flow into 50 mL tubes, utilizing the running buffer at a flow rate at 2 mL/min. Subsequently, 1.7 mL fractions of laminari-oligosaccharide mixtures were collected in a 2.2 mL V-shaped, 96 squared deep well microplate (4titude, Azenta Life Science) using a flow rate at 2 mL/min. The sizes of the laminari-oligosaccharides were analyzed with thin-layer chromatography (TLC). Distinct oligosaccharide fractions were carefully collected, lyophilized and stored at −20 °C for future utilization. The fractions were named according to their source species as follows: *L. digitata* (*Ld*), *L. hyperborea* (*Lh*) or *S. latissima* (*Sl*), with fraction indicated by a "F" and a number (e.g., *Ld*F1).

2.4.3. Thin-layer chromatography (TLC)

For a comprehensive assessment of laminari-oligosaccharides distribution and approximate sizes, 0.8 μL samples from wells 1, 4, 7, and 10 of the rows A-H of each 96 square deep well microplate containing the laminari-oligosaccharide fractions of one of three seaweed species (Figs. S1 and S2) were spotted near the bottom of the TLC silica gel (10 × 20; Merck). Close-up views were generated by spotting 2 μL on the TLC plate from the end wells in row C to E12. As a mobile phase, a mixture of 1-butanol, acetic acid, and Milli-Q water (2:1:1) was run for 1.5 h. Thereafter, the TLC plates were dried and developed using 100 mg orcinol in 95 mL methanol and 5 mL sulfuric acid. Then, the plates were dried and heated at 120 °C using the TLC Plate Heater III (CAMAG®) until bands became visible.

2.5. Structural analyses of laminarin and laminari-oligosaccharide fractions

2.5.1. Nuclear magnetic resonance (NMR) spectroscopy

1D and 2D NMR spectra were recorded on a 600 MHz Bruker Avance Neo NMR spectrometer equipped with a 5 mm TCI Prodigy CryoProbe (Bruker). Samples were dissolved in D_2O (0.5 mL, 99.9 %; Cambridge Isotope Laboratories, Tewksbury, MA, USA) and transferred to 5 mm NMR tubes. All spectra were obtained using standard Bruker pulse programs with water suppression. The 2D TOCSY spectra were recorded using an MLEV-17 mixing sequence with spin-lock times of 150 ms. The 2D NOESY spectra were recorded with a mixing time of 300 ms. Natural abundance 2D ^{13}C–^{1}H HSQC experiments were recorded without decoupling during the acquisition of the ^{1}H free induction decay. Chemical shifts were expressed in parts per million (ppm) relative to solvent HOD signal (4.84 ppm for ^{1}H NMR, 292 K). Data were processed using TopSpin™ software (Bruker). Line fitting (deconvolution) was used to estimate the average degree of polymerization, branching and G:M ratio. The expanded region (5.3–4.0 ppm) with selected peaks on the 1D ^{1}H NMR spectrum was fitted with Lorentz/Gaussian functions, to obtain the position of overlapping peaks, line widths, and integrals.

2.5.2. Matrix-assisted laser desorption/ionization time-of-flight mass spectrometry (MALDI-TOF/TOF MS)

MALDI-TOF/TOF MS experiments were performed using a Bruker ultrafleXtreme (Bruker Daltonics) mass spectrometer. All spectra were recorded in reflector positive-ion mode, and the acquisition mass range was 200–6000 Da. Samples were prepared by mixing on the target 0.5 μL sample solutions with 0.5 μL aqueous 10 % 2,5-dihydroxybenzoic acid as matrix solution.

2.5.3. Fourier transform infrared spectroscopy (FT-IR) analysis

Freeze-dried laminarin was analyzed to identify its functional groups using an FT-IR spectrometer (Nicolet iS5, Thermo Scientific) with a spectral range of 400–4000 cm^{-1}.

2.6. Laminarin and laminari-oligosaccharides effect on dendritic cells and T-cell activation

2.6.1. Sample preparation for DC-model

Lyophilized laminarin and the laminari-oligosaccharide fractions were diluted in RPMI cell culture medium (Gibco, Invitrogen, Paisley, UK), supplemented with 10 % (*v/v*) fetal calf serum (FCS; Gibco) and 1 % (*v/v*) penicillin/streptomycin (Gibco) to a stock concentration at 5 mg/mL.

2.6.2. Maturation and activation of monocyte-derived DCs

Peripheral blood mononuclear cells (PBMCs) were isolated from buffy coats of healthy donors by Ficoll Histopaque density-gradient (Sigma-Aldrich). $CD14^+$ monocytes were isolated using CD14 Microbeads (Miltenyi Biotec, Bergisch Gladbach, Germany). The $CD14^+$ monocytes were cultured in 48-well plates (Nunc) at concentration of 0.5×10^6 cells/mL for seven days in RPMI medium supplemented with FCS and antibiotics. The differentiation into immature DCs was induced with IL-4 at 12.5 ng/mL, and GM-CSF at 25 ng/mL (both from R&D Systems, Bio-Techne, Abingdon, England). Maturation of the immature DCs into mature DCs was achieved by culturing the immature DCs for 24

h in RPMI medium supplemented with FCS and antibiotics in 48-well plates at concentration of 2.5×10^5 cells/mL in the presence of IL-1β (10 ng/mL), TNFα (50 ng/mL; both from R&D Systems) and lipopolysaccharide (LPS) from *E. coli*, serotype 055:B5 (0.5 μg/mL, Sigma-Aldrich). The stock solution of 5 mg/mL of each laminarin sample was diluted in RPMI medium and added to the maturing DCs at a concentration of 100 μg/mL together with cytokines and LPS. Cells cultured with cytokines and LPS but in the absence of sample were used as negative control (Neg-DCs). After 24 h, the matured DCs were harvested and the effect of laminarin and the laminari-oligosaccharide fractions on their maturation was evaluated by measuring cytokine secretion by ELISA and expression of surface molecules by flow cytometry.

2.6.3. Co-culture of DCs and allogeneic $CD4^+$ T-cells

Allogeneic $CD4^+$ T cells were obtained from PBMCs using CD4 microbeads (Miltenyi Biotec) following the same procedure as for the isolation of $CD14^+$ monocytes described above. DCs which were matured and activated with LPS, TNFα, and IL-1β [in presence or absence of either laminarin from *L. hyperborea*, *L. hyperborea* oligosaccharide fraction *Lh*F5 or *S. latissima* oligosaccharide fraction *Sl*F3 (all at 100 μg/mL)] were co-cultured at 2×10^5 cell/mL with allogeneic $CD4^+$ T-cells at 2×10^6 cells/mL in 96-well round bottom culture plates for six days. The effects of the fractions on the ability of DCs to activate and differentiate the $CD4^+$ T-cells were determined by measuring cytokine concentrations in the co-cultures by ELISA.

2.6.4. Determination of cytokine concentrations by ELISA

The concentrations of TNFα, IL-6, IL-12p40 and IL-10 in culture supernatants from DCs and IFNγ, IL-17, IL-12p40, and IL-10 in culture supernatants from co-cultured DCs and $CD4^+$ T-cells were measured by sandwich ELISA using DuoSets from R&D Systems according to the manufacturer's protocols. To minimize the effect of variance between individuals in cytokine secretion by cultured DCs and by DCs and $CD4^+$ T-cells in co-cultures, the results are expressed as secretion index (SI). The calculations were performed by dividing the cytokine concentration (pg/mL) in the supernatant from DCs matured in the presence of a laminarin sample or in co-cultures of these DCs with $CD4^+$ T-cells, by the cytokine concentration (pg/mL) in supernatants from Neg-DCs or in co-cultures of the Neg-DCs with $CD4^+$ T-cells. Proportional index (PI) was used to evaluate the overall effect of the samples on the IL-12p40 and IL-10 cytokine secretion, calculated by dividing the SI for IL-12p40 with SI for IL-10, where $PI > 1$ was indicative of a pro-inflammatory effect and $PI < 1$ of an anti-inflammatory effect.

2.6.5. Expression of surface molecules by flow cytometry

To investigate whether laminarin and the laminari-oligosaccharide had an impact on the activation status and functional capacity of the DCs, DCs were stained with mouse monoclonal antibodies against Human Leukocyte Antigen-DR (HLA-DR; clone L243), Cluster of Differentiation (CD)40 (clone 5C3), CD14 (clone M5E2), programmed death-ligand 1 (PD-L1; CD274) (clone 5C3), and CD1c (clone L161) (all from BioLegend, Nordic Biosite, Sweden), CD141 (clone 501733; from R&D Systems), and CD86 (clone Bu63; from Bio-Rad, Watford, United Kingdom). Approximately 10,000 events gated as DCs were collected using a Sony SH800S flow cytometer (Sony Biotechnologies, UK), and the data were analyzed using Kaluza analysis software (Beckman Coulter, California, USA). Appropriate isotypic antibodies were used to evaluate background staining and set positive gates. The results are presented as percentage positive cells.

2.6.6. Viability assessment of dendritic cells

The viability of DCs exposed and not exposed to laminarin samples was analyzed by Trypan blue staining and counted by C-Chip Neubauer improved counting chamber. The percentage of viable cells was calculated by the formula provided in Eq. (1)

$$\text{Cell viability}\,(\%) = (\text{Number of viable cells})/(\text{Total number of cells}) \times 100 \quad (1)$$

2.7. Statistical analysis

Data were expressed as mean ± standard error of the mean (SEM), and statistical analysis was performed using GraphPad Prism version 10.2.1 (395) (GraphPad Software, San Diego, California, USA, www.graphpad.com). One-way ANOVA was used to compare the treated DCs with DC-Neg ($n \geq 3$) and unpaired *t*-test was used to compare co-culture experiments ($n = 6$). An asterisk indicates $p \leq 0.033$ (*), $p \leq 0.002$ (**), and $p < 0.001$ (***).

3. Results and discussion

3.1. Extraction, purification, composition analysis and capping

Laminarins from *S. latissima* and *L. hyperborea* were successfully extracted by a two-step water extraction protocol and were subsequently purified to apparent homogeneity. Firstly, the extract was treated with $CaCl_2$ to precipitate traces of alginate, then filtered through a 10 kDa membrane to remove larger molecules like fucoidan, and finally passed through a 1 kDa filter to remove smaller (degradation) products and minerals (Table 1). The laminarin % yield was 10 % and 12 % of the *L. hyperborea* and *S. latissima* biomass, respectively. In contrast, laminarin extracted from a locally sourced *L. digitata*, resulted in a low yield, likely due to a low laminarin-content present in the raw material (Table S1), while mannitol and ash content remained high after purification. To obtain *L. digitata* laminarin of good purity, commercially available laminarin (Merck) was used instead for structural analyses and

Table 1
Composition analyses of pure laminarin from *L. digitata*, *L. hyperborea* and *S. latissima*.

	L. digitata	*L. hyperborea*	*S. latissima*
Ash [% *dw*[a]]	3.90 ± 0.60	15.33 ± 0.18	15.45 ± 0.55*
TPC[b] [mg PGE/100 g lyophilized laminarin extract]	– nd[c] with NMR	– nd with NMR	1.03 ± 0.50 nd with NMR
Monosaccharide composition [% *dw*]			
Mannitol	0.42 ± 0.06	2.25 ± 0.20	4.68 ± 0.26
Fucose	0.24 ± 0.02	2.51 ± 0.02	nd
Arabinose	nd	nd	nd
Galactose	nd	0.95 ± 0.02	nd
Glucose	78.36 ± 2.17	52.86 ± 0.11	74.63 ± 4.29
Xylose	0.88 ± 0.02	0.54	nd
Mannose	1.73 ± 0.03	0.33 ± 0.07	nd
Mannuronic acid	nd	5.57 ± 0.57	nd
Guluronic acid	nd	2.19 ± 0.25	nd
Glucuronic acid	nd	0.63 ± 0.08	nd
Total uronic acids	nd	8.39 ± 0.90	nd
Total carbohydrates[d]	81.63 ± 2.30	67.83 ± 2.22	79.31 ± 4.55

The data are presented as mean value ± standard deviation (for TPC, $n = 3$ for ash, $n = 2$, and for monosaccharides, $n = 2$).
* The sample size of *S. latissima* was very low causing high standard deviation.
[a] dw means dry weight.
[b] TPC means Total Polyphenol Content.
[c] nd means not detected.
[d] Total carbohydrate is the combined amounts of neutral sugars and uronic acids.

immunomodulation tests. This laminarin product from *L. digitata* contained 78 % glucose (*w/dw*), and low levels of mannitol and ash (Table 1).

Monosugar analysis of the extracted *L. hyperborea* and *S. latissima* laminarins showed that both extracts primarily contained glucose and mannitol (Table 1). In the *S. latissima* extract, glucose constituted 75 % of the dry weight (*dw*), and mannitol made up 5 % of the *dw*, resulting in a total carbohydrate content of 80 %, with a high purity of the extracted laminarin. The extract from *L. hyperborea* was also predominantly composed of glucose (53 % *w/dw*) and mannitol (2 % *w/dw*), with minor amounts of fucose, galactose, and xylose (Table 1), implying fucoidan contamination, which was confirmed by ^{1}H NMR analysis (Fig. S3). Fucoidan was successfully removed from this sample using DEAE-cellulose anion-exchange chromatography (Fig. S3), facilitating further characterization by ^{1}H NMR and enzymatic preparation of laminari-oligosaccharides (Section 3.3).

^{1}H NMR characterization of the three chosen laminarin samples revealed coexistence of M- and G-type laminarin, with variations in the M:G ratio between the seaweed species (Fig. 1 and Table 2), consistent with existing literature [8,37]. This was observed as a chemical shift at 4.18 ppm for mannitol connected to glucose or as glucose in its α or β configuration at the reducing end (Gα/β) [(1 → 3) –β–D–Glc*p*] at δ 5.22/4.67 ppm (Fig. 1). The ratio was estimated to be 2.5:1 for the laminarins from both *L. digitata* and *S. latissima* and to be 1:1 for laminarin from *L. hyperborea* (Table 2). The M:G ratio, along with the observed mannitol content, harmonizes with literature data [8,38,39]. Comparison with the composition analysis (above) indicates that free mannitol is present in the *S. latissima* sample. Such coexistence of free mannitol has been previously reported [3,7,8], and cannot be ruled out for this study.

The total phenolic content was quantified using the TPC-assay. Phenolic content in the *L. digitata* and the *L. hyperborea* laminarin extracts was below detection levels, while *S. latissima* laminarin extract had a phenolic content of 1.03 ± 0.05 mg PGE/100 g lyophilized extract (Table 1). Although detectable, the quantity of phenolic compounds in the *S. latissima* sample was low compared to findings in other studies (5–8 g PGE/100 g lyophilized extract) [4,40].

3.2. Degree of polymerization, linkage types and branching

3.2.1. FT-IR spectroscopy for estimation of components and bond-types

FT-IR spectra of laminarin extracted from each of the three species (Fig. 2) consistently displayed characteristic absorption peaks associated with the stretching vibration of —OH groups, appearing at 3347 cm^{-1} for *L. digitata*, 3361 cm^{-1} for *L. hyperborea*, and 3314 cm^{-1} for *S. latissima*, respectively. The C—H stretching vibrations in —CH_3 or —CH_2 groups, characteristic of sugars, were observed at 2917 cm^{-1} for *L. digitata* and *L. hyperborea*, and at 2887 cm^{-1} for *S. latissima*, probably a result of variations in the laminarin structure across the species (as further described below). The pyranose absorption peak, associated with the C—H weak scissor vibration around 890 cm^{-1}, confirmed the existence of β-type glycosidic bonds for all three species. The peaks observed between 1000 and 1200 cm^{-1} were attributed to the stretching vibrations of C—C and C—O bonds in the pyranose rings, indicating polysaccharides as dominant components in the extracts. These observations agree with previously reported data [13,41].

3.2.2. Estimation of the degree of polymerization

MALDI-TOF MS analysis of the laminarins from *L. digitata*, *L. hyperborea* and *S. latissima* showed that the extracts constituted a mixture of poly- and oligosaccharides of varying sizes (Fig. 3 and Table 2). The laminarin from *L. digitata* displayed a range from DP10 to DP36, with DP25 being the dominant signal (Fig. 3). Laminarin from *L. hyperborea* exhibited a size range from DP8 to DP33, with DP24 being the dominant signal (Fig. 3), and *S. latissima* laminarin had a DP range from DP7 to DP36, with DP24 being the dominant signal (Fig. 3). This suggests an average molecular weight of approximately 5 kDa, in line with previous reported data [2–4].

3.2.3. Structural analysis of the laminarins by 1D/2D ^{1}H NMR spectroscopy

In the 1D ^{1}H NMR spectra of laminarin from *L. digitata*, *L. hyperborea*, and *S. latissima* (Fig. 1), the anomeric signals are detected at positions that correspond to the occurrence of β–1,3 and β–1,6 linkages. For the assignment of the various signals, our previously developed library of

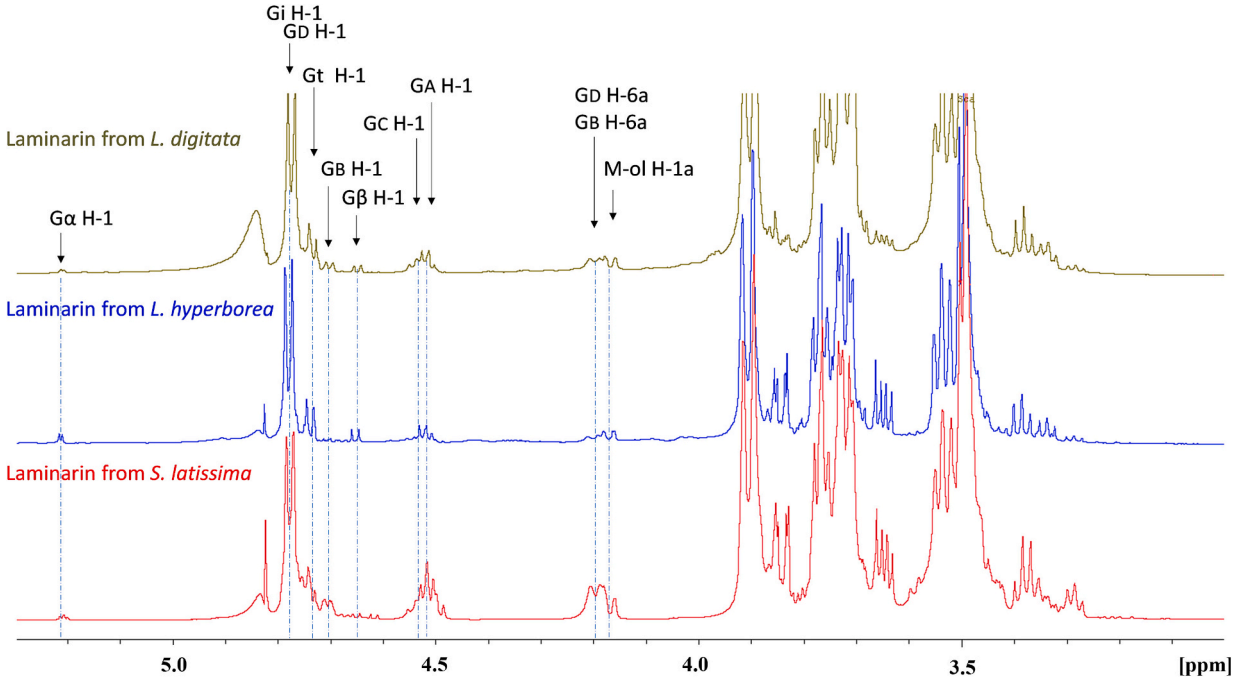

Fig. 1. ^{1}H NMR spectra of laminarin from *L. digitata*, *L. hyperborea*, and *S. latissima* highlighting possible linkages. The spectra were recorded in D_2O at 292 K. The possible linkages are shown as Gt [β-D-Glc*p*-(1 → 3)-]; Gi [−(1 → 3)-β-D-Glc*p*-(1 → 3)-]; GD [−(1 → 3,6)-β-D-Glc*p*-(1 → 3)-]; GB [−(1 → 6)-β-D-Glc*p*-(1 → 3)-]; GC [−(1 → 3)-β-D-Glc*p*-(1 → 6)-]; GA [β-D-Glc*p*-(1 → 6)-]; Gα/β (reducing end) [−(1 → 3)-β-D-Glc*p*] and M-ol [−(1 → 1)-M-ol].

Table 2
Sample overview of laminarin and laminari-oligosaccharide samples including degree of polymerization range determined by MALDI-TOF-MS, branching content, and mannitol:glucose (M:G) ratio determined with ^{1}H NMR.

Sample	Degree of polymerization	Branching	M:G chains
L. digitata laminarin	DP10–DP36, highest signal DP25	~10 % β–1,6-linkages (6.5 % branching, 3.5 % intrachain) Residues ratio GD:GB* ~2:1	~2.5:1
*Ld*F1 (well: C10-D2)[a]	DP-12–DP15	10 % β–1,6-linkage Residues ratio GD:GB 2:1	
*Ld*F2 (well: D3-D8)	DP9–DP12	7 % β–1,6-linkage Residues ratio GD:GB 2:1	
*Ld*F3 (well: D9-E1)	DP8–DP10	3 % β–1,6-branching GB residue not detected	
*Ld*F4 (well: E2-E5)	DP6–DP8	3 % β–1,6-branching GB residue not detected	
L. hyperborea laminarin	DP8–DP33, highest signal at DP24	~4 % β–1,6-branching, GB traces	~1:1
*Lh*F1 (well: C10-C12)	DP12–DP15	11 % β–1,6-branching **NB:** contamination with fucoidan	
*Lh*F2 (well: D1-D5)	DP10–DP13	7 % β–1,6-branching **NB:** contamination with fucoidan	
*Lh*F3 (well: D6-D10)	DP8–DP11	3 % β–1,6-branching	
*Lh*F4 (well: D11-E5)	DP6–DP10	3 % β–1,6-branching	
*Lh*F5 (well: E6-E7)	DP5–DP8	7 % β–1,6-branching	
S. latissima laminarin	DP7–DP36 highest signal detected at DP24	~21 % β–1,6-linkages (~15 % branching, ~6 % intrachain) Residues ratio GD:GB ~ 2:1	~2.5:1
*Sl*F1 (well: C10-D2)	DP10–DP14	20 % β–1,6-linkages (~15 % branching, ~5 % interchain) Residues ratio GD:GB ~2:1	
*Sl*F2 (well: D9-E1)	DP9–DP11	16 % β–1,6-linkages (~11 % branching, ~5 % interchain) Residues ratio GD:GB ~2:1	
*Sl*F3 (well: E2-E5)	DP6–DP9	11 % β–1,6-linkages (~7 % branching, ~4 % interchain) Residues ratio GD:GB ~2:1	

[a] Wells merged in Fig. S2.
* The GD:GB ratio reflects the β1,6-branch to β1,6-intrachain ratio.

NMR data for laminari-oligosaccharides was used (Table 3) [42,43]. Additionally, 2D ^{13}C – ^{1}H HSQC spectra were recorded confirming the assignment of chemical shifts, particularly in the bulk region, where significant overlap of signals was observed in the 1D spectrum (Fig. S4). In the 1D ^{1}H NMR spectrum, terminal *β*-D-Glc*p*-(1 → 3)-units are reflected by Gt H-1 at *δ* 4.75, internal -(1 → 3)-*β*-D-Glc*p*-(1 → 3)- units by Gi H-1 at *δ* 4.79, branching -(1 → 3,6)-*β*-D-Glc*p*-(1 → 3)- units by GD H-1 at *δ* 4.77, −(1 → 6)-*β*-D-Glc*p*-(1 → 3)- units by GB at *δ* 4.72, −(1 → 3)-*β*-D-Glc*p*-(1 → 6)- units by GC H-1 at *δ* 4.55, terminal *β*-D-Glc*p*-(1 → 6)-units by GA H-1 at *δ* 4.52, G*α*/*β* (reducing end) [−(1 → 3)-*β*-D-Glc*p*] at *δ* 5.22/4.67, respectively, and mannitol itself, which gives a M-ol H-1a signal outside the bulk region at *δ* 4.18 (Fig. 1). Due to strong overlap of the signals, line fitting (deconvolution) was used to estimate the average DP, branching and mannitol to glucose (M:G) ratio (Table 3). The percentage of the *β*–1,6-intrachain/branching in laminarin samples was estimated after integration of the GB/GD H-6a at *δ* 4.21; reducing ends: G*α*/*β* H-1 at *δ* 5.22/4.67, respectively, M-ol H-1a at *δ* 4.18 and remaining overlapping anomeric signals: Gt, Gi, GD, GC, GB, GA, respectively. The peak area of well-resolved GB H-1 signal was subtracted from the GB/GD H-6a signal, giving the percentage of GB:GD ratio. Average DP was determined by comparing the integrals of reducing ends: G*α*/*β*, M-ol signals and the integrals of overlapping anomeric signals: Gt, Gi, GD, GC, GB, GA, respectively.

The analysis highlighted distinct structural features in the laminarins from the three species. Specifically, laminarin from *S. latissima* exhibited a notable degree of branching, constituting 21 % of *β*–1,6-linkages, of which 15 % was assigned to branching and 6 % formed intrachain links, including a 1,6-branch point on the non-reducing glucose forming a kinked-linear structure (Fig. 1 and Table 2). In contrast, laminarin from *L. digitata* displayed fewer *β*–1,6-linkages compared with laminarin from *S. latissima*, with 6.5 % allocated to branching, and 3.5 % to intrachain links (Fig. 1 and Table 2). Importantly, both types of laminarin contained both longer and shorter sidechains of glucose. In contrast, laminarin from *L. hyperborea* predominantly featured a linear *β*–1,3–linked backbone with minimal branching, approximately 4 %, and lacked intrachain links (Fig. 1 and Table 2). The existing branches in *L. hyperborea* laminarin consisted solely of single glucose units, a feature that may also be influenced by various factors such as the habitats and environmental factors of the seaweed species. These results collectively affirm structural distinctions of laminarins from different brown seaweed species.

3.3. Enzymatically produced laminari-oligosaccharides

3.3.1. Structural analysis of laminari-oligosaccharides generated by LPHase

The relatively diverse bioactivities previously reported for laminarin may, partially, be attributed to distinct structural differences across brown seaweed species. These differences include elements such as branch points, intrachain links, and the distribution of *β*–1,6-linkages [44]. However, the specific structural elements responsible driving specific activities remain unclear. To address this knowledge gap, several laminari-oligosaccharide fractions from the three laminarin types, extracted and characterized above, were produced using the laminaripentaose-producing endo–1,3–*β*-glucanase, LPHase, a glycoside hydrolase family 64 enzyme. This approach enabled the creation of laminari-oligosaccharides with similar DP but with varying branching and intrachain linkage content. MALDI-TOF MS was used to determine the DP range of the laminari-oligosaccharides (Table 2), while 1D/2D ^{1}H-^{13}C NMR analyses were used to explore structural differences (Tables 2 and 3).

Laminari-oligosaccharide fractions derived from *L. hyperborea* showed an increase in *β*–1,6-branching compared to the laminarin polymer. Specifically, the oligosaccharide fraction *Lh*F1, eluting with a retention time corresponding to a higher apparent molecular weight and lower mobility on TLC (Fig. S2), contained 11 % *β*–1,6-branching, compared to 4 % in undigested laminarin. Fraction *Lh*F2 contained oligosaccharides with a somewhat lower apparent molecular weight, and showed 7 % *β*–1,6-branching (Table 2). Unfortunately, both *Lh*F1 and *Lh*F2 were contaminated with fucoidan, leading to their exclusion from immunological analysis. The two fractions, which, based on mobility, comprised intermediate-sized (*Lh*F3) and intermediate to small-sized oligosaccharides (*Lh*F4), exhibited 3 % *β*–1,6-branching, while the apparent smaller oligosaccharide fraction (*Lh*F5) contained 7 % *β*–1,6-branching, indicating an uneven distribution of the branches (Table 2). No intrachain links were observed in any of the above fractions, nor were they present in the laminarin polymer (above). The increase in branching in the oligosaccharides indicates that the short single-residue branches in *L. hyperborea* laminarin may be well accommodated in the active site of the LPHase. The enzyme is shown to have an unusually

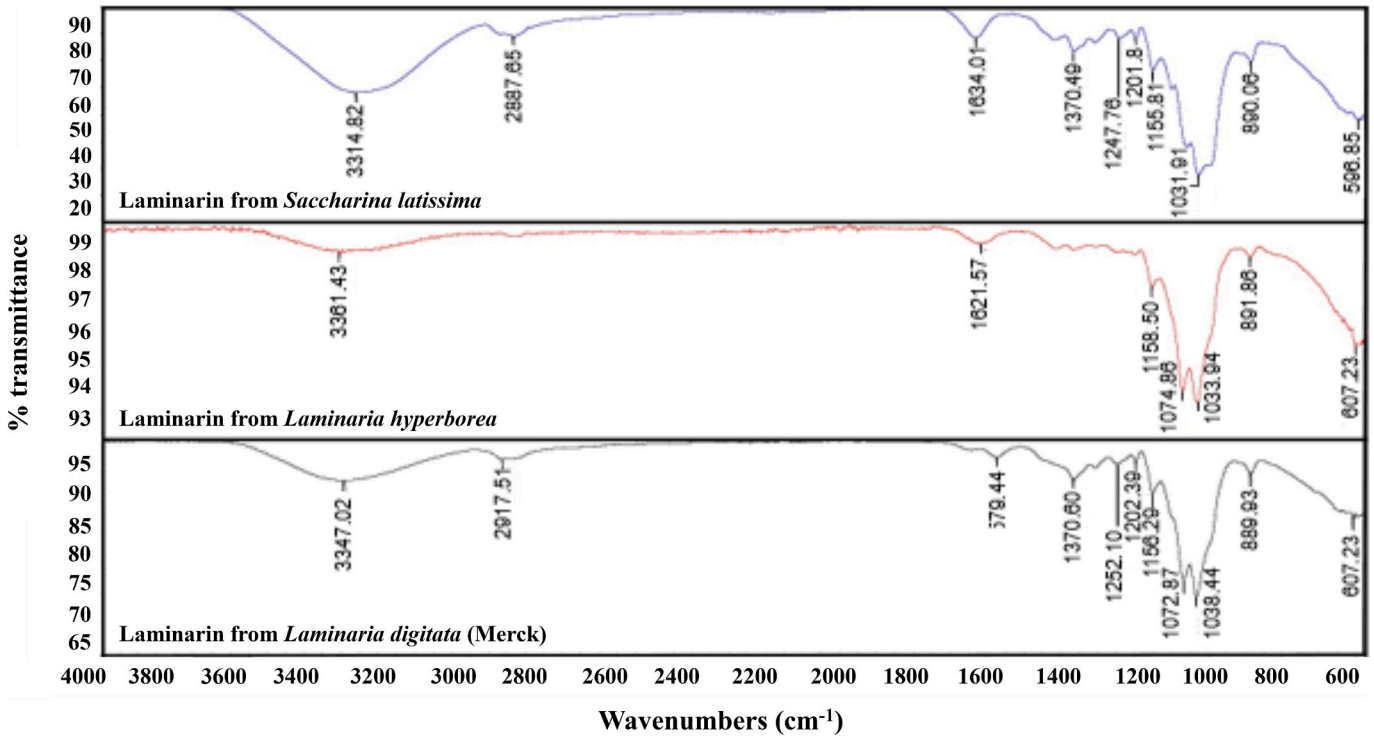

Fig. 2. FT-IR spectra of purified laminarin from *L. digitata*, *L. hyperborea* and *S. latissima*. The infrared spectra were recorded in the 400–4000 cm^{-1} region using a FT-IR system. The spectra for laminarin from *L. digitata*, *L. hyperborea* and *S. latissima* are highlighted in black, red and blue, respectively.

wide groove around the active site [45], a feature that may allow accommodation of substrates with a certain degree of branching.

In contrast, the laminarin fractions from *L. digitata* and *S. latissima* showed a gradual reduction in the percentage of *β*–1,6-linkages as the oligosaccharide mixtures decreased in their DP range (Table 2). This could suggest that the branching points occur irregularly in the polymer and that the longer branches in the polymers from these species are less accessible for substrate binding by the enzyme. For *L. digitata* laminarin, the larger oligosaccharide fractions (*Ld*F1 and *Ld*F2) contained 10 % and 7 % of the *β*–1,6-linkages, including both intrachain links and branched structures. In contrast, the intermediate and smaller oligosaccharide fractions (*Ld*F3 and *Ld*F4) each contained 3 % *β*–1,6-linkages with short side chains but without the intrachain links, indicating that these may have been hydrolyzed during the enzymatic treatment.

The *S. latissima* oligosaccharide fractions (*Sl*F1, *Sl*F2 and *Sl*F3) displayed a higher percentage of *β*–1,6-linkages (20 %, 16 %, and 11 %, respectively), reflecting the greater branching and intrachain links (21 %) of the *S. latissima* laminarin, and in *Sl*F1, maintaining the proportion found in the laminarin polymer (Table 2). Interestingly, all fractions derived from *S. latissima* contained intrachain links, indicating a higher abundance in this species [this feature was not found in the smaller oligosaccharide fractions of similar DP from *L. digitata* (*Ld*F3 and *Ld*F4)]. This indicates that the intrachain links are located closer to each other in *S. latissima*, prohibiting cleavage in the active site of LPHase.

Notably, similar to the ^{1}H NMR data from the laminarin polymer sample of *L. digitata*, citric acid was observed in all fractions from the three different species, originating from the hydrolysis with LPHase carried out using a sodium citrate buffer (data not shown). However, only traces were observed in the laminari-oligosaccharide fractions derived from *L. hyperborea*, likely due to the less branched structure of its laminarin, which results in reduced interaction with the sodium citrate buffer and the laminarin, leading to more efficient purification on the size-exclusion Superdex™ 30 HiLoad 26/600 column.

3.4. Effect of laminarin and laminari-oligosaccharide fractions on immunomodulation

3.4.1. Effect on DC maturation, cell viability and cytokine secretion

No impact on the appearance or viability of the DCs treated with laminarin or laminari-oligosaccharides for 24 h was observed compared to the non-treated control (Neg-DCs), as evidenced by their unchanged appearance under a light microscope (Fig. 4a) and viability counts exceeding 80 % in most cases (Table S2).

Maturation of the immature DCs into mature DCs was confirmed by the absence of expression of the CD14 monocyte marker and by the higher percentage of DCs expressing the antigen-presenting molecule HLA-DR, along with the co-stimulatory molecules CD40 and CD86. The expression of these molecules was not affected by treatment with any of the laminarins (Fig. 4b). In addition, laminarin treatment did not affect the expression of CD1c and CD141 on the DCs, molecules commonly used to distinguish between the DC1 and DC2 subsets [46,47], with a higher percentage of DCs expressing CD1c than CD141 (Fig. 4b). Moreover, a high percentage of DCs that expressed PD-L1 was observed, a ligand known to be upregulated upon activation (e.g., by LPS) to prevent excessive inflammation [48] (Fig. 4b), but this was not different from Neg-DCs. In summary, these results demonstrate that none of the laminarin extracts affected the maturation of the immature DCs into mature DCs.

No impact on the secretion of any of the investigated cytokines was observed when the DCs were treated with samples derived from *L. digitata* (Fig. 5a–e, light grey graphs), implying that laminarin and laminari-oligosaccharides from *L. digitata* do not promote pro- or anti-inflammatory responses in this model.

The *L. hyperborea* laminarin polymer did not affect the TNFα secretion by DCs compared to Neg-DCs, whereas DCs treated with the laminari-oligosaccharide fractions *Lh*F4 and *Lh*F5 secreted decreased levels of TNFα (35 % and 32 %, respectively; Fig. 5a, middle grey). This suggests size-dependent effect on decrease in TNFα secretion by the *L. hyperborea* laminari-oligosaccharide fractions. DCs treated with

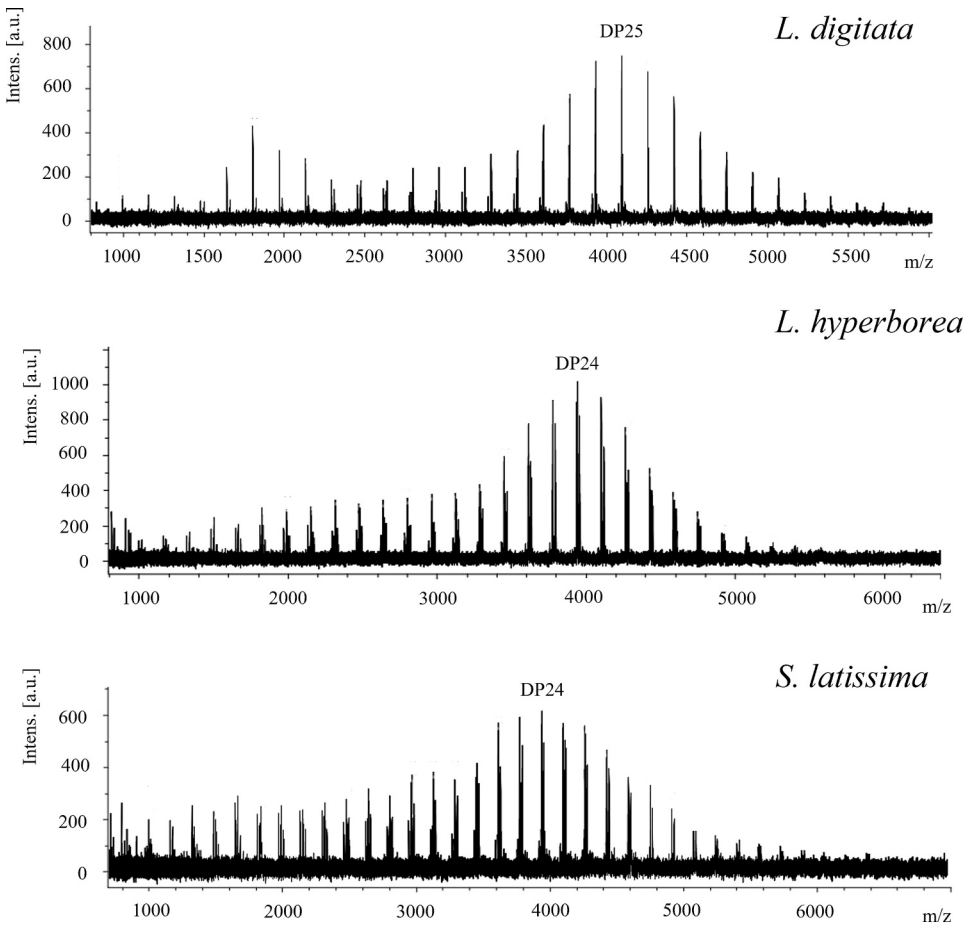

Fig. 3. MALDI-TOF MS spectra of laminarin from *L. digitata*, *L. hyperborea* and *S. latissima*. The MALDI-TOF MS spectra display the degree of polymerization composition of each extract. The dominant peaks correspond to DP25 for *L. digitata*, and DP24 for *L. hyperborea* and *S. latissima* are highlighted. These findings are consistent with the reported ranges of DP25–DP40, corresponding to molecular weights of 4.2–7.2 kDa.

laminarin from *L. hyperborea* secreted higher levels of IL-6 compared to Neg-DCs (24 %) and this was also observed for DCs treated with *Lh*F5 (34 %) (Fig. 5b, middle grey). Laminarin and laminari-oligosaccharides from *L. hyperborea* did not affect secretion of IL-12p40 (Fig. 5c, middle grey), while DCs treated with the *L. hyperborea* laminarin polymer secreted significantly higher levels of the anti-inflammatory cytokine IL-10 as compared to Neg-DCs (Fig. 5d, middle grey), resulting in a non-significant decrease in the PI by 26 % (PI < 1; Fig. 5e middle grey). Although IL-6 can induce inflammatory responses, it can, in combination with IL-10 secretion, induce anti-inflammatory response, suggesting an overall anti-inflammatory effect associated with *L. hyperborea* laminarin polymer treatment of DCs.

An 18 % decrease in TNFα secretion was observed when the DCs were treated with *Sl*F3, the smallest laminari-oligosaccharide fraction from *S. latissima* (Fig. 5a, dark grey). Treatment of DCs with laminarin and laminari-oligosaccharides from *S. latissima* did not affect the secretion of other cytokines analyzed, i.e. IL-6, IL-12p40, and IL-10, by the DCs (Fig. 5a, c and d, dark grey).

The decreased TNFα secretion by DCs is associated with the smaller fractions of laminari-oligosaccharides derived from *L. hyperborea* (*Lh*F4 and *Lh*F5) and *S. latissima* (*Sl*F3). However, it is evident that factors beyond size (DP range) may also play a role in down-regulating TNFα secretion by the DCs. This is highlighted by the observation that neither of the small laminari-oligosaccharide fractions derived from *L. digitata* (*Ld*F3 and *Ld*F4) exhibited any effect on the TNFα secretion by the DCs compared to Neg-DCs.

Results from ^{1}H NMR (Table 2) provided more detailed insights into the structural composition of the laminari-oligosaccharides. Specifically, the *Sl*F3 oligosaccharide displayed a mixture of branched and linear structures, including linear intrachain links located at the non-reducing end (Fig. S5), exhibiting a total of 11 % *β*–1,6-linkages. Conversely, the *Lh*F5 oligosaccharide primarily had linear structures with short side chains and lacked intrachain links, with an overall *β*–1,6-linkage content of 7 %. Structures similar to *Lh*F5 were found in *Ld*F3 and *Ld*F4; however, only *Lh*F5 affected TNFα secretion by the DCs. A plausible explanation for this difference in secretion is that a specific percentage of *β*–1,6-linkages may be necessary to influence TNFα secretion by the DCs, as the laminari-oligosaccharide fractions *Ld*F3 and *Ld*F4, which had no effect, only contained 3 % *β*–1,6-linkages. Both *Sl*F3 and *Lh*F5 affected TNFα secretion by the DCs, but while *Sl*F3 included both branches and intrachain links, *Lh*F5 was lacking the latter, potentially linking the effect on TNFα secretion to the *β*–1,6-branching rather than intrachain links in the laminari-oligosaccharides.

The absence of intrachain links, combined with the presence of small branches may also affect the IL-10 secretion by DCs. The *L. hyperborea* laminarin polymer, characterized by approximately 4 % *β*–1,6-linkages (Table 2), is devoid of intrachain links, but caused an increase in IL-10 secretion by the DCs, a phenomenon not observed with the other two laminarin polymers that contain the intrachain structures (Fig. S5). Thus, the simple branching pattern, primarily consisting of short side chains, of laminarin from *L. hyperborea* may play a significant role in its effect on IL-10 secretion by DCs.

The ^{1}H NMR data revealed the presence of citric acid in all fraction samples, likely originating from the LPHase digestion method. Therefore, the effect of sodium citrate buffer on cytokine secretion by DCs was assessed. No significant effects were observed on TNFα, IL-6, IL-12p40,

Table 3
^{1}H and ^{13}C NMR chemical shifts (δ) of *L. digitata*, *L. hyperborea*, S. *latissima*, recorded in D_2O at 292 K.

	Residue	H-1a/ 1b C-1	H-2 C-2	H-3 C-3	H-4 C-4	H-5 C-5	H-6a/ 6b C-6
Gα	-(1 → 3)-α-D-Glc*p*	5.22 93.0	3.73 72.0	3.92 83.3	3.52 70.0	3.86 72.2	3.83/ 3.79 61.6
Gβ	-(1 → 3)-β-D-Glc*p*	4.67 96.6	3.44 74.9	3.74 85.7	3.52 69.2	3.49 76.6	3.90/ 3.74 61.6
G2α	-(1 → 3)-β-D-Glc*p*-(1 → 3)-α-D-Glc*p*	4.76 103.7	3.56 74.3	3.78 85.3	3.54 69.1	3.52 76.7	3.93/ 3.74 61.7
G2β	-(1 → 3)-β-D-Glc*p*-(1 → 3)-β-D-Glc*p*	4.77 103.7	3.56 74.3	3.78 85.3	3.53 69.1	3.53 76.7	3.93/ 3.74 61.7
G2	-(1 → 3)-β-D-Glc*p*-(1 → 1)-D-Man-ol	4.54 103.6	3.56 73.9	3.74 85.3	3.54 69.1	3.52 76.6	3.92/ 3.76 61.7
Gi	-(1 → 3)-β-D-Glc*p*-(1 → 3)-	4.79 103.4	3.56 73.9	3.77 85.5	3.54 69.1	3.52 76.6	3.92/ 3.76 61.7
Gt	β-D-Glc*p*-(1 → 3)-	4.75 103.7	3.37 74.4	3.53 76.6	3.42 70.6	3.48 76.8	3.92/ 3.72 61.7
GA	β-D-Glc*p*-(1 → 6)-	4.52 103.7	3.32 74.0	3.51 76.0	3.41 70.6	3.46 76.7	3.92/ 3.74 61.6
GB	-(1 → 6)-β-D-Glc*p*-(1 → 3)-	4.72 103.8	3.38 74.4	3.53 76.5	3.48 70.5	3.67 75.6	4.21/ 3.87 69.7
GC	-(1 → 3)-β-D-Glc*p*-(1 → 6)-	4.55 103.6	3.52 73.6	3.74 85.6	3.51 69.1	3.50 76.6	3.92/ 3.75 61.6
GD	-(1 → 3,6)-β-D-Glc*p*-(1 → 3)-	4.77 103.8	3.60 74.0	3.79 85.4	3.58 69.1	3.69 75.4	4.21/ 3.89 69.7
M-ol	-(1 → 1)-D-Man-ol	4.18/ 3.84 72.6	3.87 70.6	3.85 n.d.	3.75 71.7	3.79 70.0	3.86/ 3.67 64.0

n.d. = not determine.

or IL-10 (Fig. S6), confirming that the alterations in cytokine secretion by DCs treated with laminarins can be attributed to the polymer or oligomers of the laminarins rather than by the buffer.

As TNFα is a key pro-inflammatory cytokine involved in the initiation and progression of acute inflammatory responses, important in protecting the body against harmful effects of pathogens and damaged tissues [26]. However, in autoimmune diseases, such as inflammatory bowel disease, rheumatoid arthritis, and psoriasis [49,50], dysregulated TNFα production becomes a hallmark of pathogenesis, driving chronic inflammation and exacerbating tissue injury [27,51]. Thus, treatments that decrease TNFα secretion by DCs, such as by *Lh*F5 and *Sl*F3, could potentially ameliorate inflammatory conditions and autoimmune diseases by reducing TNFα secretion, minimizing tissue damage and inflammation [53]. Similarly, the increase in IL-10 secretion by DCs treated with the laminarin polymer from *L. hyperborea* indicates anti-inflammatory properties, as IL-10 plays an important role in limiting excessive immune responses [52]. In summary, these data suggest that the laminarin polymer from *L. hyperborea* and the small oligosaccharide fractions *Lh*F5 and *Sl*F3 may be beneficial as treatment of excessive inflammation as observed in many chronic inflammatory diseases.

3.4.2. Effect on DCs and T-cell crosstalk

Given the key role of DCs in not only activating naïve T cells but also in directing their differentiation, the impact of DCs matured for 24 h in the presence of laminarin from *L. hyperborea*, and the laminari-oligosaccharides *Lh*F5 or *Sl*F3 on cytokine secretion when co-cultured with allogeneic $CD4^+$ T-cells was investigated. Secretion of IFN-γ and IL-17 was examined as indicators of Th1 and Th17 responses, respectively, while IL-10 can be secreted by both the DCs, to stimulate T-regulatory (Treg) cells [52,53], or by the $CD4^+$ T-cells themselves, suggesting a Treg cell response (as reviewed [54,55]). IL-12p40 is reported to be secreted only by DCs in the co-culture [56].

When DCs were matured in the presence of laminarin from *L. hyperborea* and subsequently co-cultured with allogeneic $CD4^+$ T-cells, a significant increase in both IL-17 and IL-10 secretion was observed (Fig. 6a). This indicates a complex interplay between *L. hyperborea* laminarin-treated DCs and allogeneic $CD4^+$ T-cells in modulating the immune response. The increased IL-17 concentration in the co-culture supernatant may result from the increased IL-6 secretion by laminarin-treated DCs (Fig. 5b), as IL-6 is one of the main cytokines inducing Th17 differentiation of naïve T cells [57]. This suggests that laminarin from *L. hyperborea* may play a role in type 3 immune response, which is characteristic of immunity against extracellular bacteria and fungi [58,59]. The increase in IL-10 was similar to what was observed when DCs were cultured in the presence of laminarin from *L. hyperborea* (Fig. 5d, middle grey). The increase in IL-10 secretion in the co-culture supernatant might result from DC secretion, as DCs treated with laminarin from *L. hyperborea* secreted elevated levels of IL-10; however, it can also be derived from the $CD4^+$ T-cells. In either case, the high levels of IL-10 secretion suggest a regulatory role of laminarin, most likely within the adaptive immune system.

When *Lh*F5-treated DCs were co-cultured with allogeneic $CD4^+$ T-cells, a non-significant decrease in IFN-γ secretion and IL-12p40 secretion was observed compared to untreated DCs co-cultured with allogeneic $CD4^+$ T-cells (Fig. 6b). In contrast, when DCs matured in the presence of *Sl*F3 were co-cultured with allogeneic $CD4^+$ T-cells, a significant decrease in IFN-γ, IL-12p40, and IL-10 secretions by 26 %, 16 %, and 38 %, respectively, was observed (Fig. 6c). The decrease in IL-12p40 and IFN-γ secretion observed in response to *Sl*F3 treatment suggests a decrease in type 1 immune response, as IL-12 is the main cytokine inducing Th1 differentiation of naïve T cells [60], which is characteristic of immunity against intracellular bacteria [58,59]. Although decreased IL-10 secretion on its own may point toward a pro-inflammatory response, the data was in line with previous results that have shown that reduction in IL-10 secretion in combination with decreased IL-12p40 secretion leads to lower IFN-γ secretion [61,62].

4. Conclusions

In this study, laminarins were isolated and purified from two species of brown seaweed, *L. hyperborea* and *S. latissima*, using a two-step water extraction process, while laminarin from *L. digitata* was sourced commercially. Laminari-oligosaccharides were generated from the purified laminarins through digestion with LPHase, enabling structural analysis that revealed differences and similarities among the laminarins and their laminari-oligosaccharide fractions in *β–1,3(1,6)*-linkages and DP.

Treating DCs with laminarin from *L. hyperborea* increased IL-6 secretion and resulted in elevated IL-17 secretion when the treated DCs were co-cultured with allogeneic $CD4^+$ T-cells, suggesting a promotion of type 3 immune responses, which may be beneficial against extracellular pathogens. Furthermore, DCs treated with small, simply branched oligosaccharides without intrachain links from *L. hyperborea* (*Lh*F4 and *Lh*F5) and the more complex-structured small oligosaccharides fraction from *S. latissima* (*Sl*F3) secreted reduced levels of TNFα without affecting their IL-12p40 secretion. When the DCs treated with *Lh*F5 or *Sl*F3 were co-cultured with allogeneic $CD4^+$ T-cells effects were observed on type 1 immune response. The effects were marked for *Sl*F3. As type 1 immune response is linked to chronic inflammation, these data suggest that the small oligosaccharides fractions from *L. hyperborea* (*Lh*F5) and *S. latissima* (*Sl*F3) might be useful as therapeutics against chronic inflammatory diseases.

However, these promising data also highlight challenges to be

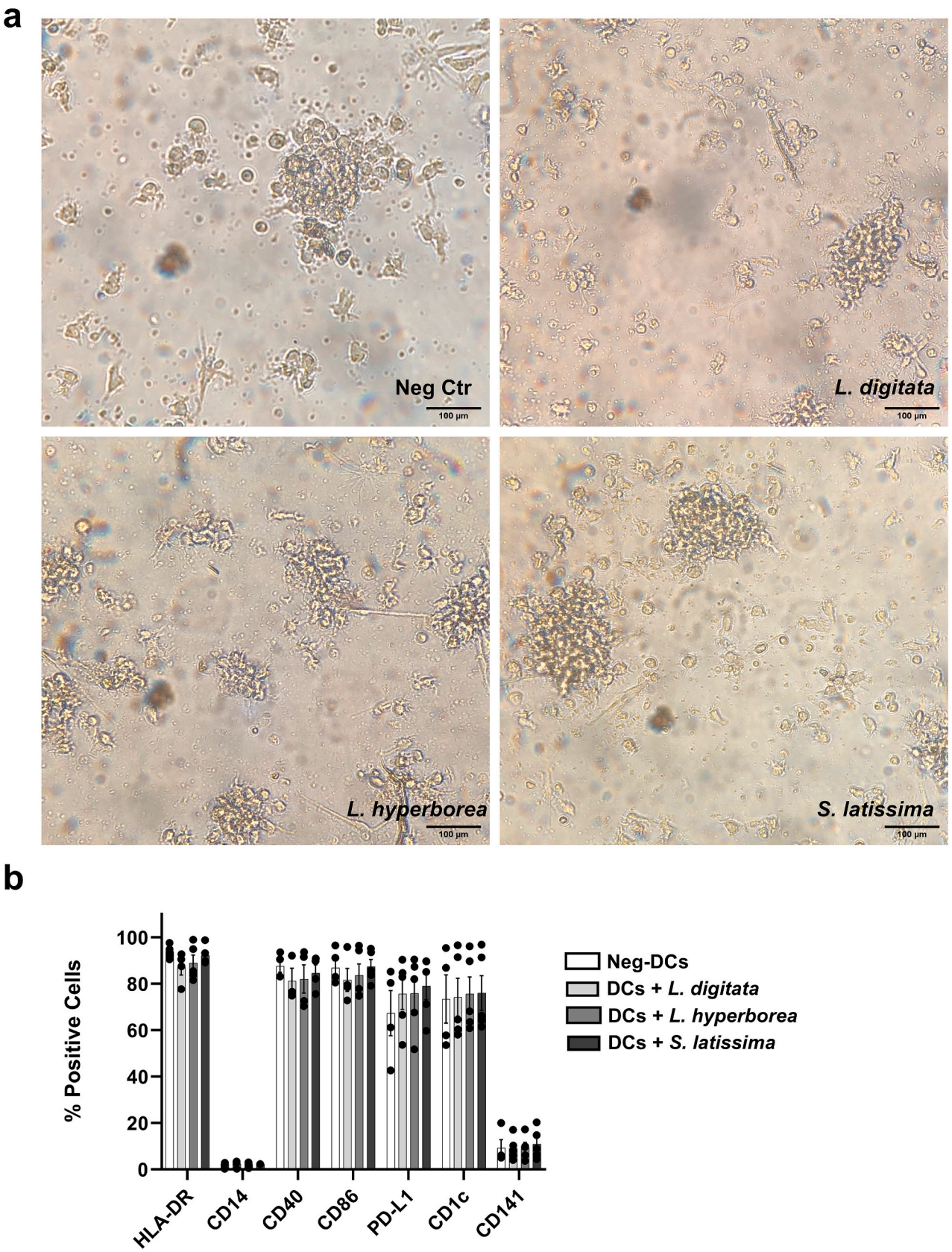

Fig. 4. The impact of laminarin on dendritic cell (DC) maturation and activation. The maturation and activation of DCs were assessed through light microscopy and flow cytometry analysis. (a) Representative images of mature DCs in the absence (Neg Ctr) or presence of laminarin from *L. digitata*, *L. hyperborea* or *S. latissima* after 24 h incubation. Arrows indicate mature DCs. Images were captured using a Leica DMLS light microscope equipped with a Cplan 10×/0.22 objective. (b) Expression of surface molecules crucial for mature DC function following laminarin supplementation is displayed. Results are presented as mean ± SEM of percentage positive cells, with individual data points shown ($n = 4$). The DCs were treated for 24 h without (Neg-DCs) or with laminarin from *L. digitata*, *L. hyperborea* and *S. latissimi*.

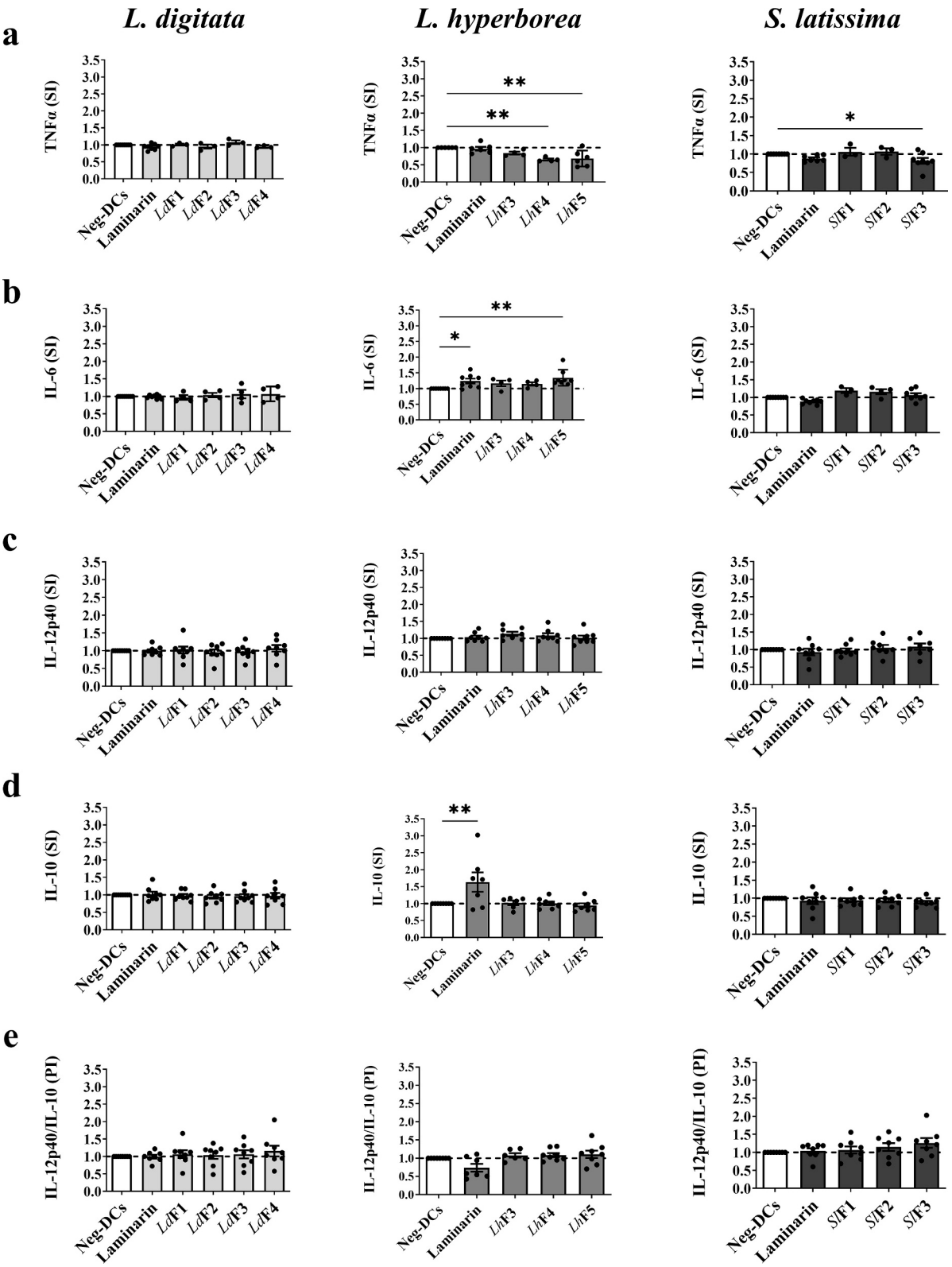

Fig. 5. Effect of laminarin and laminari-oligosaccharides on cytokine secretion by mature dendritic cells (DCs). Cytokine secretion indexes (SI) of TNFα (a), IL-6 (b), IL-12p40 (c), and IL-10 (d), as well as the proportional indexes (PI) between IL-12p40 and IL-10 (e), are shown for mature DCs treated with of laminarin or laminari-oligosaccharides fractions from *L. digitata* (Light grey), *L. hyperborea* (middle grey) and *S. latissima* (dark grey), respectively, compared to the mature DCs without experimental treatment (Neg-DCs). In each graph, treatments labeled as "laminarin" represent laminarin derived from the species specified on top of the images, while the respective oligosaccharide fractions are marked with an "F" followed by a number. All samples were given in a concentration at 100 μg/mL. Experimental treatments were compared to the Neg-DCs using one-way ANOVA with Dunnett's post hoc test in GraphPad Prism version 10.2.1 (395) Significance markers in the results are denoted as follows: * for $p \leq 0.033$, ** for $p \leq 0.002$, and *** for $p < 0.001$. Sample sizes ranged from $n = 3$–8.

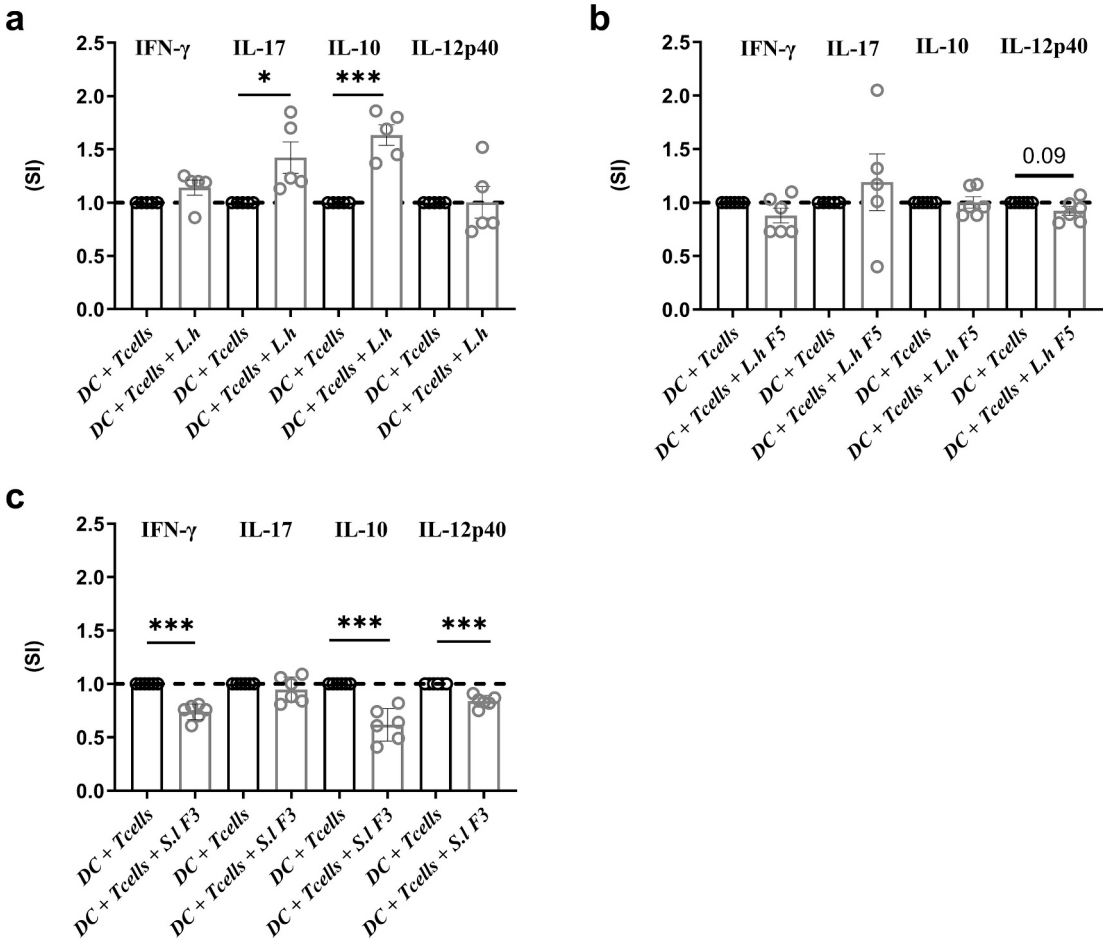

Fig. 6. Cytokine secretion indexes in cultures of dendritic cell (DCs) co-cultured with allogeneic $CD4^+$ T-cells after treatment with laminarin or laminari-oligosaccharides. The cytokine secretion of IFNγ, IL-17, IL-10 and IL-12p40 in supernatants of DCs co-cultured with allogeneic $CD4^+$ T-cells ($CD4^+$T) were measured and presented in as secretion indexes (SI). The DCs were matured either without or with laminarin from *L. hyperborea*, or with the fractions *Lh*F5 or *Sl*F3, at a concentration of 100 μg/mL for 24 h, before being co-cultured with allogeneic $CD4^+$ T cells. The label DC + $CD4^+$ T refers to DCs without treatment co-cultured with allogeneic $CD4^+$ T cells and DC + Laminarin (a), *Lh*F5 (b), or *Sl*F3 (c) indicate DCs treated with one of the samples for 24 h. The DC:$CD4^+$ T cell ratio was 1:10. Cytokine secretion was quantified by ELISA. Results are presented as mean ± SEM of secretion indexes (SI) of IFNγ, IL-17, IL-10 and IL-12p40 (n = 5–6). Experimental treatments were compared to the DC + $CD4^+$ T by unpaired *t*-test in GraphPad Prism version 10.2.1 (395). Significance markers in the results are denoted as follows: * for $p \leq 0.033$, ** for $p \leq 0.002$, and *** for $p < 0.001$, n = 5–6.

addressed in future research. The variability in laminarin yield and purity from different seaweed species underscores the need for standardized extraction and purification protocols, as the structural features resulting in biological activity may need fine-tuning, as was found for *S. latissima* laminarin, where only certain oligosaccharides resulted in bioactivity. This calls for further work, to fully elucidate the bioactivity mechanisms. This study also provided detailed data on structural analysis and immunomodulatory effects of laminarins and their oligosaccharides, with the observed effects on DCs and T-cell interactions assessed in a controlled in vitro environment. This may, however, not completely reflect the complexities of in vivo immune responses, or the influence of other biological factors present in a living organism. Thus, investigations of the bioavailability, metabolism, and safety of laminarins and their oligosaccharide derivatives in animal models are also necessary to confirm their therapeutic potential and address possible adverse effects.

This work shows that laminarins from brown seaweeds have potential as immune-modulating compounds, both in fighting infections and treating chronic inflammation but that detailed selection of the structure is necessary to obtain the desired effect.

Supplementary data to this article can be found online at https://doi.org/10.1016/j.ijbiomac.2025.141287.

CRediT authorship contribution statement

Monica Daugbjerg Christensen: Writing – review & editing, Writing – original draft, Visualization, Methodology, Investigation, Formal analysis, Data curation. **Leila Allahgholi:** Writing – review & editing, Visualization, Formal analysis, Data curation. **Justyna M. Dobruchowska:** Writing – review & editing, Investigation, Formal analysis, Data curation. **Antoine Moenaert:** Data curation. **Hörður Guðmundsson:** Writing – review & editing, Formal analysis, Data curation. **Ólafur Friðjónsson:** Writing – review & editing, Supervision. **Eva Nordberg Karlsson:** Writing – review & editing, Supervision, Funding acquisition. **Guðmundur Ó. Hreggviðsson:** Writing – review & editing, Supervision, Funding acquisition, Conceptualization. **Jona Freysdottir:** Writing – review & editing, Supervision, Funding acquisition.

Institutional review board statement

Not applicable.

Funding

This research was funded by the MARIKAT JPI Cofund Blue Bio-Economy project (grant number 9082-00021B), European Union's Horizon Europe program SeaMark (Seaweed-based market applications) project (grant number 101060379), and Landspitali Science Fund (grants number A-2020-034, A-2021-027 and A-2022-025).

Declaration of competing interest

The authors declare that they have no known competing financial interests or personal relationships that could have appeared to influence the work reported in this paper.

Acknowledgments

Not applicable.

Data availability

The data presented in this study are available upon request from the corresponding author.

References

[1] T.M. Thompson, B.R. Young, S. Baroutian, Advances in the pretreatment of brown macroalgae for biogas production, Fuel Process. Technol. 195 (2019) 106–151, https://doi.org/10.1016/j.fuproc.2019.106151.
[2] S.E. Spicer, J.M.M. Adams, D.S. Thomas, J.A. Gallagher, A.L. Winters, Novel rapid method for the characterisation of polymeric sugars from macroalgae, J. Appl. Phycol. 29 (2017) 1507–1513, https://doi.org/10.1007/s10811-016-0995-0.
[3] L.E. Rioux, S.L. Turgeon, M. Beaulieu, Characterization of polysaccharides extracted from brown seaweeds, Carbohydr. Polym. 69 (2007) 530–537, https://doi.org/10.1016/j.carbpol.2007.01.009.
[4] S.U. Kadam, C.P. O'Donnell, D.K. Rai, M.B. Hossain, C.M. Burgess, D. Walsh, B. K. Tiwari, Laminarin from Irish brown seaweeds Ascophyllum nodosum and Laminaria hyperborea: ultrasound assisted extraction, characterization and bioactivity, Mar. Drugs 13 (2015) 4270–4280, https://doi.org/10.3390/md13074270.
[5] Z. Liu, Y. Xiong, L. Yi, R. Dai, Y. Wang, M. Sun, X. Shao, Z. Zhang, S. Yuan, Endo-β-1,3-glucanase digestion combined with the HPAEC-PAD-MS/MS analysis reveals the structural differences between two laminarins with different bioactivities, Carbohydr. Polym. 194 (2018) 339–349, https://doi.org/10.1016/j.carbpol.2018.04.044.
[6] D. Wang, D.H. Kim, E.J. Yun, Y.C. Park, J.H. Seo, K.H. Kim, The first bacterial β-1,6-endoglucanase from Saccharophagus degradans 2-40T for the hydrolysis of pustulan and laminarin, Appl. Microbiol. Biotechnol. 101 (2017) 197–204, https://doi.org/10.1007/s00253-016-7753-8.
[7] S.U. Kadam, B.K. Tiwari, C.P. O'Donnell, Extraction, structure and biofunctional activities of laminarin from brown algae, Int. J. Food Sci. Technol. 50 (2015) 24–31, https://doi.org/10.1111/ijfs.12692.
[8] S.M. Read, G. Currie, A. Bacic, Analysis of the structural heterogeneity of laminarin by electrospray-ionisation-mass spectrometry, Carbohydr. Res. 281 (1996) 187–201.
[9] A.M. Neyrinck, A. Mouson, N.M. Delzenne, Dietary supplementation with laminarin, a fermentable marine β (1–3) glucan, protects against hepatotoxicity induced by LPS in rat by modulating immune response in the hepatic tissue, Int. Immunopharmacol. 7 (2007) 1497–1506, https://doi.org/10.1016/j.intimp.2007.06.011.
[10] J. Il Choi, H.J. Kim, J.H. Kim, J.W. Lee, Enhanced biological activities of laminarin degraded by gamma-ray irradiation, J. Food Biochem. 36 (2012) 465–469, https://doi.org/10.1111/j.1745-4514.2011.00552.x.
[11] A.J. Smith, B. Graves, R. Child, P.J. Rice, Z. Ma, D.W. Lowman, H.E. Ensley, T. Ryter, J.T. Evans, D.L. Williams, Immunoregulatory activity of the natural product laminarin varies widely as a result of its physical properties, J. Immunol. 200 (2018) 788–799, https://doi.org/10.4049/jimmunol.1701258.
[12] K.H. Kim, Y.W. Kim, H.B. Kim, B.J. Lee, D.S. Lee, Anti-apoptotic activity of laminarin polysaccharides and their enzymatically hydrolyzed oligosaccharides from Laminaria japonica, Biotechnol. Lett. 28 (2006) 439–446, https://doi.org/10.1007/s10529-005-6177-9.
[13] G. Rajauria, R. Ravindran, M. Garcia-Vaquero, D.K. Rai, T. Sweeney, J. O'Doherty, Molecular characteristics and antioxidant activity of laminarin extracted from the seaweed species Laminaria hyperborea, using hydrothermal-assisted extraction and a multi-step purification procedure, Food Hydrocoll. 112 (2021) 106332, https://doi.org/10.1016/j.foodhyd.2020.106332.
[14] R.V. Menshova, S.P. Ermakova, S.D. Anastyuk, V.V. Isakov, Y.V. Dubrovskaya, M. I. Kusaykin, B. Um, T.N. Zvyagintseva, Structure, enzymatic transformation and anticancer activity of branched high molecular weight laminaran from brown alga Eisenia bicyclis, Carbohydr. Polym. 99 (2014) 101–109, https://doi.org/10.1016/j.carbpol.2013.08.037.
[15] Y. Huang, H. Jiang, X. Mao, F. Ci, Laminarin and laminarin oligosaccharides originating from brown algae: preparation, biological activities, and potential applications, J. Ocean Univ. China 20 (2021) 641–653, https://doi.org/10.1007/s11802-021-4584-8.
[16] S.M. Tosh, P.J. Wood, Q. Wang, J. Weisz, Structural characteristics and rheological properties of partially hydrolyzed oat β-glucan: the effects of molecular weight and hydrolysis method, Carbohydr. Polym. 55 (2004) 425–436, https://doi.org/10.1016/j.carbpol.2003.11.004.
[17] K.L. Cheong, J.K. Li, S. Zhong, Preparation and structure characterization of high-value Laminaria digitata oligosaccharides, Front. Nutr. 9 (2022), https://doi.org/10.3389/fnut.2022.945804.
[18] N. Jayapala, V. Toragall, G.K. Gnanesh, S.R. Chaudhari, V. Baskaran, Preparation, characterization, radical scavenging property and antidiabetic potential of laminarioligosaccharides derived from laminarin, Algal Res. 63 (2022) 102642, https://doi.org/10.1016/j.algal.2022.102642.
[19] O. Joffre, M.A. Nolte, R. Spörri, C.R.E. Sousa, Inflammatory signals in dendritic cell activation and the induction of adaptive immunity, Immunol. Rev. 227 (2009) 234–247, https://doi.org/10.1111/j.1600-065X.2008.00718.x.
[20] M. Cabeza-Cabrerizo, A. Cardoso, C.M. Minutti, M. Pereira Da Costa, C. Reis E. Sousa, Dendritic cells revisited, Annu. Rev. Immunol. 39 (2021) 131–166, https://doi.org/10.1146/annurev-immunol-061020-053707.
[21] F. Annunziato, C. Romagnani, S. Romagnani, The 3 major types of innate and adaptive cell-mediated effector immunity, J. Allergy Clin. Immunol. 135 (2015) 626–635, https://doi.org/10.1016/j.jaci.2014.11.001.
[22] G.E. Kaiko, J.C. Horvat, K.W. Beagley, Immunological decision-making : how does the immune system decide to mount a helper T-cell response ? Immunology 123 (2008) 326–338, https://doi.org/10.1111/j.1365-2567.2007.02719.x.
[23] L. Zhou, I.I. Ivanov, R. Spolski, R. Min, K. Shenderov, T. Egawa, D.E. Levy, W. J. Leonard, D.R. Littman, IL-6 programs TH-17 cell differentiation by promoting sequential engagement of the IL-21 and IL-23 pathways, Nat. Immunol. 8 (2007) 967–974, https://doi.org/10.1038/ni1488.
[24] S. Hirohata, T. Yanagida, Human Thl responses driven by IL-12 are associated with enhanced expression of CD40 ligand, Jpn. J. Clin. Immunol. 21 (1998) 67–76, https://doi.org/10.2177/jsci.21.supplement_67.
[25] C.A. Hunter, S.A. Jones, IL-6 as a keystone cytokine in health and disease, Nat. Immunol. 16 (2015) 448–457, https://doi.org/10.1038/ni.3153.
[26] D.I. Jang, A.H. Lee, H.Y. Shin, H.R. Song, J.H. Park, T.B. Kang, S.R. Lee, S.H. Yang, The role of tumor necrosis factor alpha (Tnf-α) in autoimmune disease and current tnf-α inhibitors in therapeutics, Int. J. Mol. Sci. 22 (2021) 1–16, https://doi.org/10.3390/ijms22052719.
[27] D.R. Germolec, K.A. Shipkowski, R.P. Frawley, E. Evans, Markers of inflammation, in: Methods in Molecular Biology, Humana Press Inc., 2018, pp. 57–79, https://doi.org/10.1007/978-1-4939-8549-4_5.
[28] F. Ghorbaninezhad, P. Leone, H. Alemohammad, B. Najafzadeh, N.S. Nourbakhsh, M. Prete, E. Malerba, H. Saeedi, N.J. Tabrizi, V. Racanelli, B. Baradaran, Tumor necrosis factor-α in systemic lupus erythematosus: structure, function and therapeutic implications (review), Int. J. Mol. Med. 49 (2022), https://doi.org/10.3892/IJMM.2022.5098.
[29] S.K. Mittal, P.A. Roche, Suppression of antigen presentation by IL-10, Curr. Opin. Immunol. 34 (2015) 22–27, https://doi.org/10.1016/j.coi.2014.12.009.
[30] P.J. Murray, The primary mechanism of the IL-10-regulated antiinflammatory response is to selectively inhibit transcription, Proc. Natl. Acad. Sci. 102 (2005) 8686–8691, https://doi.org/10.1073/pnas.0500419102.
[31] M. Nakabayashi, T. Nishijima, G. Ehara, N. Nikaidou, H. Nishihashi, T. Watanabe, Structure of the gene encoding laminaripentaose-producing β-1,3-glucanase (LPHase) of Streptomyces matensis DIC-108, J. Ferment. Bioeng. 85 (1998) 459–464.
[32] A.D. Premarathna, T.A.E. Ahmed, A. Sooäär, V. Rjabovs, A.T. Critchley, M. T. Hincke, R. Tuvikene, Extraction and functional characterization of fucoidans and alginates from Ecklonia maxima: a focus on skin, immune, and intestinal health, Food Hydrocoll. 159 (2025), https://doi.org/10.1016/j.foodhyd.2024.110668.
[33] V.L. American Society of Enologists, J.A. Rossi, American Journal of Enology and Viticulture, in: Am J Enol Vitic, American Society of Enologists, 1965, pp. 144–158.
[34] A. Sluiter, B. Hames, R. Ruiz, C. Scarlata, J. Sluiter, D. Templeton, Determination of Ash in Biomass, Laboratory Analytical Procedure (LAP), 2008, p. 8.
[35] A. Sluiter, B. Hames, R. Ruiz, C. Scarlata, J. Sluiter, D. Templeton, D. Crocker, Determination of Structural Carbohydrates and Lignin in Biomass, Technical Report NREL/ TP -510 -42618, 2008, pp. 1–15, doi:NREL/TP-510-42618.
[36] H. Motejadded, J. Altenbuchner, Construction of a dual-tag system for gene expression, protein affinity purification and fusion protein processing, Biotechnol. Lett. 31 (2009) 543–549, https://doi.org/10.1007/s10529-008-9909-9.
[37] A.O. Chizhov, A. Dell, H.R. Morris, A.J. Reason, S.M. Haslam, R.A. Mcdowell, O.S. Chizhov, A.I. Usov, Structural Analysis of Laminarans by MALDI and FAB Mass Spectrometry, (n.d.).
[38] A. Graiff, W. Ruth, U. Kragl, U. Karsten, Chemical characterization and quantification of the brown algal storage compound laminarin — a new methodological approach, J. Appl. Phycol. 28 (2016) 533–543, https://doi.org/10.1007/s10811-015-0563-z.
[39] L. Allahgholi, R.R.R. Sardari, S. Hakvåg, K.Z.G. Ara, T. Kristjansdottir, I.M. Aasen, O.H. Fridjonsson, T. Brautaset, G.O. Hreggvidsson, E.N. Karlsson, Composition analysis and minimal treatments to solubilize polysaccharides from the brown

seaweed Laminaria digitata for microbial growth of thermophiles, J. Appl. Phycol. 32 (2020) 1933–1947, https://doi.org/10.1007/s10811-020-02103-6.
[40] T. Wang, R. Jónsdóttir, G. Ólafsdóttir, Total phenolic compounds, radical scavenging and metal chelation of extracts from Icelandic seaweeds, Food Chem. 116 (2009) 240–248, https://doi.org/10.1016/j.foodchem.2009.02.041.
[41] C.F. Ji, Y. Bin Ji, D.Y. Meng, Sulfated modification and anti-tumor activity of laminarin, Exp. Ther. Med. 6 (2013) 1259–1264, https://doi.org/10.3892/etm.2013.1277.
[42] J.M.M. Dobruchowska, Jon O. Jonsson, Olafur H. Fridjonsson, Arnthor Aevarsson, Jakob K. Kristjansson, Josef Altenbuchner, Hildegard Watzlawick, Gerrit J. Gerwig, Lubbert Dijkhuizen, Johannis P. Kamerling, Gudmundur O. Hreggvidsson, Modification of linear (β1→3)-linked gluco-oligosaccharides with a novel recombinant 2 β-glucosyltransferase (trans-β-glucosidase) enzyme from Bradyrhizobium diazoefficiens, Glycobiology 26 (2016) 1157–1170.
[43] G.O. Hreggvidsson, J.M. Dobruchowska, O.H. Fridjonsson, J.O. Jonsson, G. J. Gerwig, A. Aevarsson, J.K. Kristjansson, D. Curti, R.R. Redgwell, C.E. Hansen, J. P. Kamerling, T. Debeche-Boukhit, Exploring novel non-Leloir β-glucosyltransferases from proteobacteria for modifying linear (β1→3)-linked gluco-oligosaccharide chains, Glycobiology 21 (2011) 304–328, https://doi.org/10.1093/glycob/cwq165.
[44] E.L. Adams, P.J. Rice, B. Graves, H.E. Ensley, H. Yu, G.D. Brown, S. Gordon, M. A. Monteiro, E. Papp-Szabo, D.W. Lowman, T.D. Power, M.F. Wempe, D. L. Williams, Differential high-affinity interaction of Dectin-1 with natural or synthetic glucans is dependent upon primary structure and is influenced by polymer chain length and side-chain branching, J. Pharmacol. Exp. Ther. 325 (2008) 115–123, https://doi.org/10.1124/jpet.107.133124.
[45] H.M. Wu, S.W. Liu, M.T. Hsu, C.L. Hung, C.C. Lai, W.C. Cheng, H.J. Wang, Y.K. Li, W.C. Wang, Structure, mechanistic action, and essential residues of a GH-64 enzyme, laminaripentaose-producing β-1,3-glucanase, J. Biol. Chem. 284 (2009) 26708–26715, https://doi.org/10.1074/jbc.M109.010983.
[46] M. Collin, V. Bigley, Human dendritic cell subsets: an update, Immunology 154 (2018) 3–20, https://doi.org/10.1111/imm.12888.
[47] G. Breton, S. Zheng, R. Valieris, I. Tojal, R. Satija, M.C. Nussenzweig, Human dendritic cells (DCs) are derived from distinct circulating precursors that are precommitted to become CD1c+ or CD141+ DCs, J. Exp. Med. 213 (2016) 2861–2870, https://doi.org/10.1084/jem.20161135.
[48] Q. Peng, X. Qiu, Z. Zhang, S. Zhang, Y. Zhang, Y. Liang, J. Guo, H. Peng, M. Chen, Y. Fu, H. Tang, PD-L1 on dendritic cells attenuates T cell activation and regulates response to immune checkpoint blockade, Nat. Commun. 11 (2020) 1–8, https://doi.org/10.1038/s41467-020-18570-x.
[49] S.O. Adegbola, K. Sahnan, J. Warusavitarne, A. Hart, P. Tozer, Anti-TNF therapy in Crohn's disease, Int. J. Mol. Sci. 19 (2018), https://doi.org/10.3390/ijms19082244.
[50] U. Müller-Ladner, T. Pap, R.E. Gay, M. Neidhart, S. Gay, Mechanisms of disease: the molecular and cellular basis of joint destruction in rheumatoid arthritis, Nat. Clin. Pract. Rheumatol. 1 (2005) 102–110, https://doi.org/10.1038/ncprheum0047.
[51] K.P. Kumar, A.J. Nicholls, C.H.Y. Wong, Partners in crime: neutrophils and monocytes/macrophages in inflammation and disease, Cell Tissue Res. 371 (2018) 551–565, https://doi.org/10.1007/s00441-017-2753-2.
[52] A.J. Kassianos, M.Y. Hardy, X. Ju, D. Vijayan, Y. Ding, A.J.E. Vulink, K. J. Mcdonald, S.L. Jongbloed, R.B. Wadley, C. Wells, D.N.J. Hart, K.J. Radford, Human CD1c (BDCA-1) + myeloid dendritic cells secrete IL-10 and display an immuno-regulatory phenotype and function in response to Escherichia coli, Eur. J. Immunol. 42 (2012) 1512–1522, https://doi.org/10.1002/eji.201142098.
[53] M. Saraiva, A. O'Garra, The regulation of IL-10 production by immune cells, Nat. Rev. Immunol. 10 (2010) 170–181, https://doi.org/10.1038/nri2711.
[54] M.G. Roncarolo, S. Gregori, M. Battaglia, R. Bacchetta, K. Fleischhauer, M. K. Levings, Interleukin-10-secreting type 1 regulatory T cells in rodents and humans, Immunol. Rev. 212 (2006) 28–50, https://doi.org/10.1111/j.0105-2896.2006.00420.x.
[55] C.M. Hawrylowicz, A. O'Garra, Potential role of interleukin-10-secreting regulatory T cells in allergy and asthma, Nat. Rev. Immunol. 5 (2005) 271–283, https://doi.org/10.1038/nri1589.
[56] X. Ma, W. Yan, H. Zheng, Q. Du, L. Zhang, Y. Ban, N. Li, F. Wei, Regulation of IL-10 and IL-12 production and function in macrophages and dendritic cells, F1000Res 4 (2015) 1–13, https://doi.org/10.12688/f1000research.7010.1.
[57] L. Guglani, S.A. Khader, Th17 cytokines in mucosal immunity and inflammation, Curr. Opin. HIV AIDS 5 (2010) 120–127, https://doi.org/10.1097/COH.0b013e328335c2f6.
[58] H. Ishigame, S. Kakuta, T. Nagai, M. Kadoki, A. Nambu, Y. Komiyama, N. Fujikado, Y. Tanahashi, A. Akitsu, H. Kotaki, K. Sudo, S. Nakae, C. Sasakawa, Y. Iwakura, Differential roles of interleukin-17A and -17F in host defense against mucoepithelial bacterial infection and allergic responses, Immunity 30 (2009) 108–119, https://doi.org/10.1016/j.immuni.2008.11.009.
[59] L. Lin, A.S. Ibrahim, X. Xu, J.M. Farber, V. Avanesian, B. Baquir, Y. Fu, S. W. French, J.E. Edwards, B. Spellberg, Th1-Th17 cells mediate protective adaptive immunity against Staphylococcus aureus and Candida albicans infection in mice, PLoS Pathog. 5 (2009), https://doi.org/10.1371/journal.ppat.1000703.
[60] M.K. Gately, L.M. Renzetti, J. Magram, A.S. Stern, L. Adorini, U. Gubler, D. H. Presky, The Interleukin-12/ Interleukin-12-receptor System: Role in Normal and Pathologic Immune Responses, 1998.
[61] J. Freysdottir, M.B. Sigurpalsson, S. Omarsdottir, E.S. Olafsdottir, A. Vikingsson, I. Hardardottir, Ethanol extract from birch bark (Betula pubescens) suppresses human dendritic cell mediated Th1 responses and directs it towards a Th17 regulatory response in vitro, Immunol. Lett. 136 (2011) 90–96, https://doi.org/10.1016/j.imlet.2010.12.009.
[62] V. Kale, J. Freysdottir, B.S. Paulsen, Ó.H. Friojónsson, G. Óli Hreggviosson, S. Omarsdottir, Sulphated polysaccharide from the sea cucumber Cucumaria frondosa affect maturation of human dendritic cells and their activation of allogeneic CD4(+) T cells in vitro, Bioact. Carbohydr. Diet. Fibre 2 (2013) 108–117, https://doi.org/10.1016/j.bcdf.2013.09.009.